Electron Donor-Acceptor (EDA) Complex Mediated Visible-Light Driven Sulfur–Fluorine Bond Reduction of Pentafluorosulfanyl Arenes Using Potassium Iodide

Tatsuhiro Uchikura, Fua Akutsu and Takahiko Akiyama

Department of Chemistry, Faculty of Science, Gakushuin University, 1-5-1, Mejiro, Toshima-ku, Tokyo 171-8588, Japan

Email: takahiko.akiyama@gakushuin.ac.jp

Contents | Page

1. General Methods

All operations were performed under nitrogen unless otherwise noted. NMR spectra for products data (^{1}H and ^{13}C) were recorded on a Bruker AVANCE-III (400 MHz for ^{1}H, 100 MHz for ^{13}C, 376 MHz for ^{19}F) and JEOL ECZ-400 (400 MHz for ^{1}H, 101 MHz for ^{13}C, 376 MHz for ^{19}F, 149 MHz for ^{119}Sn, 80 MHz for ^{127}I) spectrometer using $CDCl_3$ [tetramethylsilane (0 ppm) served as an internal standard in ^{1}H NMR and $CDCl_3$ (77.0 ppm) in ^{13}C NMR, 4-fluoroanisole (−124.6 ppm) served as an internal standard in ^{19}F NMR]. Chemical shifts are expressed in parts per million (ppm). ESI mass analyses were performed on Bruker micrOTOF mass spectrometer. IR spectra were recorded on a FT/IR-4200 (JASCO Co., Ltd.). UV-Vis spectra were recorded on a V-670 UV–VIS–NIR spectrometer (JASCO Co., Ltd.). Cyclic Voltammetry was performed on ALS Model612E Electrochemical Analyzer (BAS Inc.). Visible light irradiation was performed with PR160L-467 nm (Kessil Co., Ltd.) for 467 nm LED and LED450-100STND (Optcode Co., Ltd.) for 450 nm blue LED.

Solvents were distilled according to the usual procedures and stored over molecular sieves unless otherwise noted. All of the substrates were purified by distillation (for liquid) or recrystallization (for solid). Other chemicals were purchased and used as received.

2. Screening of conditions

Table S1. Screening of conditions

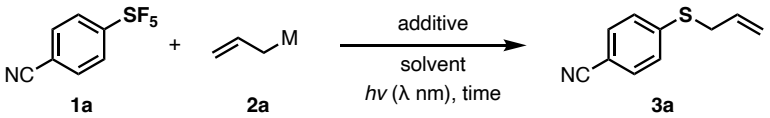

entry	M	solvent	additive	time	λ	yield
1	$SnBu_3$	THF	LiI (20 equiv), Et_3N (1.0 equiv)	24 h	467	82% (74%)
2	$SnBu_3$	THF	LiI (3.0 equiv), Et_3N (1.0 equiv)	24 h	467	45%
3	$SnBu_3$	THF	LiI (1.0 equiv), Et_3N (1.0 equiv)	24 h	467	30%
4	$SnBu_3$	THF	LiI (20 equiv), Et_3N (1.0 equiv)	6 h	467	61%
5	Bpin	THF	LiI (20 equiv), Et_3N (1.0 equiv)	24 h	467	22%
6	$SnBu_3$	THF	LiI (20 equiv)	24 h	467	82% (81%)
7	$SnBu_3$	THF	LiI (3.0 equiv)	24 h	467	45%
8	$SnBu_3$	DMF	LiI (3.0 equiv)	24 h	467	(63%)
9	$SnBu_3$	THF	LiCl (3.0 equiv)	24 h	467	0%
10	$SnBu_3$	THF	LiBr (3.0 equiv)	24 h	467	0%
11	$SnBu_3$	THF	$LiClO_4$ (3.0 equiv)	24 h	467	0%
12	$SnBu_3$	THF	$LiBF_4$ (3.0 equiv)	24 h	467	0%
13	$SnBu_3$	DMF	LiI (20 equiv)	24 h	467	(71%)
14	$SnBu_3$	MeCN	LiI (20 equiv)	24 h	467	50%
15	$SnBu_3$	Et_2O	LiI (20 equiv)	24 h	467	46%
16	$SnBu_3$	1,4-dioxane	LiI (20 equiv)	24 h	467	0%
17	$SnBu_3$	MeOH	LiI (20 equiv)	24 h	467	0%
18	$SnBu_3$	DMF	LiI (6.0 equiv)	24 h	467	57%
19	$SnBu_3$	DMF	NaI (6.0 equiv)	24 h	467	73% (75%)
20	$SnBu_3$	DMF	MgI_2 (6.0 equiv)	24 h	467	67% (68%)
21	$SnBu_3$	DMF	KI (6.0 equiv)	24 h	467	79% (78%)
22	$SnBu_3$	DMF	CaI_2 (6.0 equiv)	24 h	467	73% (70%)
23	$SnBu_3$	DMF	$^nBu_4NI$ (6.0 equiv)	24 h	467	24%
24	$SnBu_3$	THF	I_2 (6.0 equiv)	24 h	467	0%
25	$SnBu_3$	DMF	CuI (6.0 equiv)	24 h	467	<10%
26	$SnBu_3$	DMF	NiI_2 (6.0 equiv)	24 h	467	0%
27	$SnBu_3$	DMF	CoI_2 (6.0 equiv)	24 h	467	0%
28	$SnBu_3$	DMF	KBr (6.0 equiv)	24 h	467	0%
29	$SnBu_3$	DMF	KCl (6.0 equiv)	24 h	467	0%
30	$SnBu_3$	DMF	KBF_4 (6.0 equiv)	24 h	467	0%
31	$SnBu_3$	DMF	KIO_4 (6.0 equiv)	24 h	467	0%
32	$SnBu_3$	DMF	KI (6.0 equiv)	24 h	427	55%
33	$SnBu_3$	DMF	KI (6.0 equiv)	24 h	390	<31%
34	$SnBu_3$	DMF	KI (10 mol%)	24 h	467	<10%

3. Synthetic Procedures and Characterization of New Compounds

General procedure of reduction of trifluoromethylarene (Procedure I)

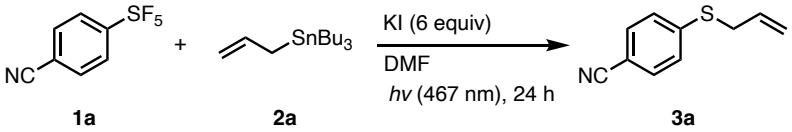

In a dried test tube, **1a** (22.9 mg, 0.10 mmol), **2a** (93.0 μL, 0.30 mmol) and KI (99.6 mg, 0.60 mmol) were mixed in DMF (2 mL), and degassed three times by the freeze-pump-thaw. The mixture was irradiated with 467 nm blue LED for 24 h. After the irradiation, water was added to the mixture and extracted with ethyl acetate for 3 times. The combined organic phase was dried over Na_2SO_4 and the solvent was removed *in vacuo* by rotary evaporator and resulting DMF was removed by smart evaporator C1 (BioChromato Co., Ltd.). The crude mixture was purified by preparative TLC on SiO_2 (hexane: diethyl ether = 4 : 1) to give **3a** (13.7 mg, 0.078 mmol) in 78%. The reactions using other substrates in Figure 2 were performed based on this Procedure I.

Data of products

3a	Colorless oil, 13.7 mg, 78%
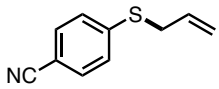	^{1}H NMR (400 MHz, $CDCl_3$) δ 7.52 (d, *J* = 8.5 Hz, 2H), 7.32 (d, *J* = 8.5 Hz, 2H), 5.87 (ddt, *J* = 16.8, 10.1, 6.6 Hz, 1H), 5.28 (ddt, *J* = 17.0, 1.4, 1.4 Hz, 1H), 5.18 (ddt, *J* = 10.0, 1.2, 1.2 Hz, 1H), 3.63 (ddd, *J* = 6.5, 1.4, 1.2 Hz, 2H).
	^{13}C NMR (101 MHz, $CDCl_3$) δ 144.1, 132.2, 127.5, 118.9, 108.5, 35.2.
	LRMS (ESI): [M+Na]+ Calcd for $C_{10}H_9NNaS$: 198.04, Found 198.04
	HRMS (ESI): [M+Na]+ Calcd for $C_{10}H_9NNaS$: 198.0353, Found 198.0350
	IR (neat, cm^{-1}): 2225, 1594, 1487, 1220, 1089, 772.

3b	Yellow solid, 15.7 mg, 81%
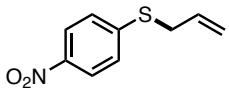	^{1}H NMR (400 MHz, $CDCl_3$) δ 8.16 – 8.10 (m, 2H), 7.37 – 7.32 (m, 2H), 5.89 (ddt, *J* = 16.7, 10.0, 6.4 Hz, 1H), 5.36 – 5.28 (m, 1H), 5.21 (ddt, *J* = 10.1, 1.4, 1.4 Hz, 1H), 3.68 (ddd, *J* = 6.5, 1.4, 1.4 Hz, 2H).
	^{13}C NMR (100 MHz, $CDCl_3$) δ 146.8, 144.9, 131.8, 126.5, 123.7, 118.9, 34.9.
	LRMS (ESI): [M+Na]+ Calcd for $C_9H_9NNaO_2S$: 218.03, Found 218.03
	HRMS (ESI): [M+Na]+ Calcd for $C_9H_9NNaO_2S$: 218.0252, Found 218.0255
	IR (neat, cm^{-1}): 1578, 1510, 1337, 1090.

3c	White solid, 10.2 mg, 49%
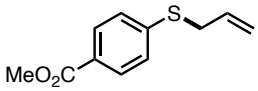	^{1}H NMR (400 MHz, $CDCl_3$) δ 7.97 – 7.89 (m, 2H), 7.35 – 7.27 (m, 2H), 5.89 (ddt, *J* = 16.9, 10.1, 6.7 Hz, 1H), 5.26 (ddt, *J* = 17.2, 1.7, 1.6 Hz, 1H), 5.15 (ddt, *J* = 10.0, 1.3, 1.3 Hz, 1H), 3.90 (s, 3H), 3.67 – 3.59 (m, 2H).
	^{13}C NMR (101 MHz, $CDCl_3$) δ 166.8, 143.2, 132.6, 129.8, 127.1, 127.0, 118.4, 52.0, 35.5.
	LRMS (ESI): [M+Na]+ Calcd for $C_{11}H_{12}NaO_2S$: 231.05, Found 231.05
	HRMS (ESI): [M+Na]+ Calcd for $C_{11}H_{12}NaO_2S$: 231.0456, Found 231.0454
	IR (neat, cm^{-1}): 1718, 1595, 1435, 1285, 1111, 772.

3d	Yellow solid, 4.3 mg, 22%
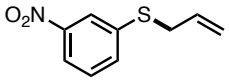	^{1}H NMR (400 MHz, $CDCl_3$) δ 8.14 (t, *J* = 2.0 Hz, 1H), 8.03 – 7.99 (m, 1H), 7.62 – 7.57 (m, 1H), 7.44 (t, *J* = 8.0 Hz, 1H), 5.87 (ddt, *J* = 16.9, 10.0, 6.8 Hz, 1H), 5.23 (ddt, *J* = 17.0, 1.4, 1.4 Hz, 1H), 5.15 (ddt, *J* = 10.0, 1.1, 1.1 Hz, 1H), 3.64 (d, *J* = 6.8 Hz, 2H).
	^{13}C NMR (101 MHz, $CDCl_3$) δ 148.4, 139.0, 134.6, 132.4, 129.4, 123.1, 120.7, 118.8, 36.4.
	LRMS (ESI): [M+Na]+ Calcd for $C_9H_9NNaO_2S$: 218.03, Found 218.03
	HRMS (ESI): [M+Na]+ Calcd for $C_9H_9NNaO_2S$: 218.0252, Found 218.0254
	IR (neat, cm^{-1}): 1636, 1525, 1348, 1127, 925, 750, 730.

4b	Colorless oil, 12.0 mg, 63%
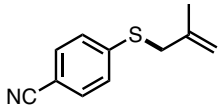	^{1}H NMR (400 MHz, $CDCl_3$) δ 7.51 (d, *J* = 8.5 Hz, 2H), 7.32 (d, *J* = 8.5 Hz, 2H), 4.98 (s, 1H), 4.92 (s, 1H), 3.60 (s, 2H), 1.85 (s, 3H).
	^{13}C NMR (101 MHz, $CDCl_3$) δ 144.5, 139.5, 132.1, 127.6, 118.9, 114.8, 108.4, 39.8, 21.2.
	LRMS (ESI): [M+H]+ Calcd for $C_{11}H_{12}NS$: 190.07, Found 190.07
	HRMS (ESI): [M+H]+ Calcd for $C_{11}H_{12}NS$: 190.0690, Found 190.0692
	IR (neat, cm^{-1}): 2225, 1593, 1486, 1089, 772.

4c	Colorless oil, 10.9 mg, 58%
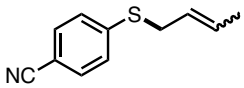	^{1}H NMR (400 MHz, $CDCl_3$; 51:49 *E*/*Z* mixture) δ 7.55 – 7.49 (m, 2H), 7.34 – 7.27 (m, 2H), 5.80 – 5.64 (m, 2H), 5.58 – 5.44 (m, 2H), 3.65 (dt, *J* = 7.5, 1.1, 1.1 Hz, 2H), 3.58 (dt, *J* = 6.8, 1.2, 1.2 Hz, 2H), 1.73 – 1.66 (m, 6H).
	^{13}C NMR (101 MHz, $CDCl_3$; 51:49 *E*/*Z* mixture) δ 144.8, 144.7, 132.2, 132.1, 130.3, 129.1, 127.4, 127.3, 124.7, 124.0, 119.0, 118.9, 108.3, 108.2, 34.5, 29.1, 17.8, 13.0.
	LRMS (ESI): [M+Na]+ Calcd for $C_{11}H_{11}NNaS$: 212.05, Found 212.05
	HRMS (ESI): [M+Na]+ Calcd for $C_{11}H_{11}NNaS$: 212.0510, Found 212.0508
	IR (neat, cm^{-1}): 2225, 1593, 1486, 1220, 1089, 773.

4d	Colorless oil, 11.3 mg, 56%
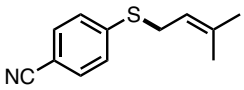	^{1}H NMR (400 MHz, $CDCl_3$) δ 7.54 – 7.49 (m, 2H), 7.32 – 7.27 (m, 2H), 5.28 (ddt, *J* = 9.0, 6.1, 1.4 Hz, 1H), 3.61 (d, *J* = 7.6 Hz, 2H), 1.74 (d, *J* = 0.4 Hz, 3H), 1.70 (s, 3H).
	^{13}C NMR (101 MHz, $CDCl_3$) δ 145.3, 137.9, 132.1, 127.1, 119.0, 117.8, 108.1, 30.4, 25.7, 17.9.
	LRMS (ESI): [M+Na]+ Calcd for $C_{12}H_{13}NNaS$: 226.07, Found 226.07
	HRMS (ESI): [M+Na]+ Calcd for $C_{12}H_{13}NNaS$: 226.0666, Found 226.0667
	IR (neat, cm^{-1}): 2225, 1592, 1486, 1089, 821, 772.

4e	White solid, 8.3 mg, 33%
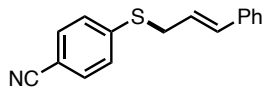	^{1}H NMR (400 MHz, $CDCl_3$) δ 7.57 – 7.50 (m, 2H), 7.41 – 7.34 (m, 2H), 7.34 – 7.22 (m, 5H), 6.59 (d, *J* = 15.8 Hz, 1H), 6.23 (dt, *J* = 15.8, 7.0 Hz, 1H), 3.81 (dd, *J* = 7.0, 1.3 Hz, 2H).
	^{13}C NMR (101 MHz, $CDCl_3$) δ 144.0, 136.2, 133.9, 132.2, 128.6, 128.0, 127.7, 126.4, 123.4, 118.8, 108.6, 35.1.
	LRMS (ESI): [M+Na]+ Calcd for $C_{16}H_{13}NNaS$: 274.07, Found 274.07
	HRMS (ESI): [M+Na]+ Calcd for $C_{16}H_{13}NNaS$: 274.0666, Found 274.0664
	IR (neat, cm^{-1}):2224, 1590, 1486, 1220, 1087, 772.

4f[S1]	White solid, 11.9 mg, 53%
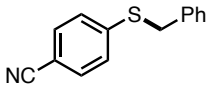	^{1}H NMR (400 MHz, $CDCl_3$) δ 7.50 (d, *J* = 8.6 Hz, 2H), 7.39 – 7.27 (m, 7H), 4.20 (s, 2H).
	^{13}C NMR (101 MHz, $CDCl_3$) δ 144.4, 135.7, 132.2, 128.8, 128.7, 127.7, 127.3, 118.8, 108.5, 37.0.

4g	White solid, 14.5 mg, 60%
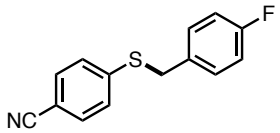	^{1}H NMR (400 MHz, $CDCl_3$) δ 7.55 – 7.48 (m, 2H), 7.36 – 7.28 (m, 4H), 7.05 – 6.97 (m, 2H), 4.17 (s, 2H).
	^{13}C NMR (101 MHz, $CDCl_3$) δ 162.2 (d, *J* = 246.8 Hz), 144.0, 132.3, 131.4 (d, *J* = 3.3 Hz), 130.3 (d, *J* = 8.2 Hz), 127.5, 118.7, 115.7 (d, *J* = 21.6 Hz), 108.8, 36.4.
	^{19}F NMR (376 MHz, $CDCl_3$) δ -93.6 (t, *J* = 14.9 Hz), -108.6 – -108.9 (m).
	LRMS (ESI): [M+Na]+ Calcd for $C_{14}H_{10}FNNaS$: 266.04, Found 266.04
	HRMS (ESI): [M+Na]+ Calcd for $C_{14}H_{10}FNNaS$: 266.0416, Found 266.0414
	IR (neat, cm^{-1}): 2224, 1594, 1508, 1216, 1090, 772.

4h	White solid, 12.8 mg, 46%
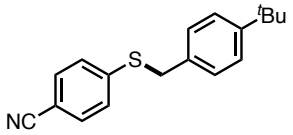	^{1}H NMR (400 MHz, $CDCl_3$) δ 7.53 – 7.48 (m, 2H), 7.38 – 7.27 (m, 6H), 4.18 (s, 2H), 1.31 (s, 9H).
	^{13}C NMR (101 MHz, $CDCl_3$) δ 150.8, 144.9, 132.5, 132.2, 128.4, 127.0, 125.7, 118.9, 108.3, 36.6, 34.5, 31.3.
	LRMS (ESI): [M+Na]+ Calcd for $C_{18}H_{19}NNaS$: 304.11, Found 304.11
	HRMS (ESI): [M+Na]+ Calcd for $C_{18}H_{19}NNaS$: 304.1136, Found 304.1135
	IR (neat, cm^{-1}): 2227, 1594, 1486, 1220, 1087, 772.

4i	White solid, 6.9 mg, 29%
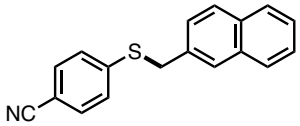	^{1}H NMR (400 MHz, $CDCl_3$) δ 7.88 – 7.75 (m, 4H), 7.56 – 7.45 (m, 5H), 7.37 – 7.31 (m, 2H), 4.36 (s, 2H).
	^{13}C NMR (101 MHz, $CDCl_3$) δ 144.3, 133.2, 133.1, 132.7, 132.2, 128.7, 127.70, 127.68, 127.48, 127.47, 126.48, 126.45, 126.2, 118.8, 108.6, 37.4.
	LRMS (ESI): [M+Na]+ Calcd for $C_{18}H_{13}NNaS$: 298.07, Found 298.07
	HRMS (ESI): [M+Na]+ Calcd for $C_{18}H_{13}NNaS$: 298.0666, Found 298.0668
	IR (neat, cm^{-1}): 2223, 1507, 1398, 1220, 772.

4j	White solid, 12.6 mg, 73%
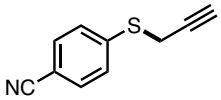	^{1}H NMR (400 MHz, $CDCl_3$) δ 7.62 – 7.56 (m, 2H), 7.46 – 7.40 (m, 2H), 3.70 (d, J = 2.6 Hz, 2H), 2.27 (t, J = 2.6 Hz, 1H).
	^{13}C NMR (101 MHz, $CDCl_3$) δ 142.7, 132.3, 127.5, 118.7, 109.2, 78.4, 72.2, 20.7.
	LRMS (ESI): [M+Na]+ Calcd for $C_{10}H_7NNaS$: 196.02, Found 196.02
	HRMS (ESI): [M+Na]+ Calcd for $C_{10}H_7NNaS$: 196.0197, Found 196.0198
	IR (neat, cm^{-1}): 3235, 2925, 2852, 2225, 1594, 1488, 1402, 1261, 1092, 809, 771.

1 mmol scale experiment

In a dried Schlenk flask, **1b** (249 mg, 1.0 mmol), **2a** (0.93 mL, 3.0 mmol) and KI (996 mg, 6.0 mmol) were mixed in DMF (20 mL), and degassed five times by the freeze-pump-thaw. The mixture was irradiated with two 467 nm blue LED for 72 h. After the irradiation, water was added to the mixture and extracted with ethyl acetate for 3 times. The combined organic phase was dried over Na_2SO_4 and the solvent was removed *in vacuo* by rotary evaporator and resulting DMF was removed by smart evaporator C1 (BioChromato Co., Ltd.). The crude mixture was purified by preparative TLC on SiO_2 (hexane: diethyl ether = 4 : 1) to give **3b** (127 mg, 0.65 mmol) in 65%.

4. Mechanistic study

4-1. Measurement of quantum yield

4-1-1. Measurement of photon flux[S2]

The photon flux of this blue LED was determined by standard ferrioxalate actinometry. The ferrioxalate solution was prepared by $K_3[Fe(C_2O_4)_3]\bullet 3H_2O$ (2.21 g) dissolving in degassed 0.05 M H_2SO_4 aq. (30 mL). The buffered phenanthroline solution was prepared by 1,10-phenanthroline (50 mg) and sodium acetate (11.25 g) dissolving in degassed 0.5 M H_2SO_4 aq. (50 mL).

The ferrioxalate solution (2.0 mL) in the reaction vessel was irradiated for 1 s or 2 s, and the buffered phenanthroline solution (1.0 mL) was added. The non-irradiated ferrioxalate solution was also treated under the same conditions (as t = 0 sample). This mixture was left to stand for 30 min, followed by diluted 8 times with distilled water. The concentrations of $Fe(phen)_3^{2+}$ were measured by UV–Vis spectra.

The conversion of Fe^{3+} into Fe^{2+} was calculated using:

$$mol\ Fe^{2+} = \frac{V \cdot \Delta A_{510\ nm}}{l \cdot \varepsilon}$$

[V: total volume of solution (0.003 × 8 L), $\Delta A_{510\ nm}$: difference in the absorbance at λ = 510 nm between irradiated and non-irradiated solutions, l: path length (1.0 cm), ε: molar absorptivity of $Fe(phen)_3^{2+}$ at 510 nm (11000 $L\bullet mol^{-1}\bullet cm^{-1}$)].

The mol/s Fe^{2+} was calculated by the slope of the plotted line to 6.32×10^{-7} $mol\bullet s^{-1}$.

The photon flux (I) was calculated using:

$$I = \frac{mol/s\ Fe^{2+}}{\Phi_{Fe}(1 - 10^{-A_{450\ nm}})}$$

[Φ_{Fe}: quantum yield of the ferrioxalate actinometer for 0.15 M solution at 458 nm (0.845), $A_{450\ nm}$: absorbance of the ferrioxalate solution at 450 nm (2.01)]

$$I = \frac{6.32 \times 10^{-7}}{0.845 \times (1 - 10^{-2.01})} = 7.55 \times 10^{-7}\ [mol \cdot s^{-1}]$$

4-1-2. Calculation of quantum yield

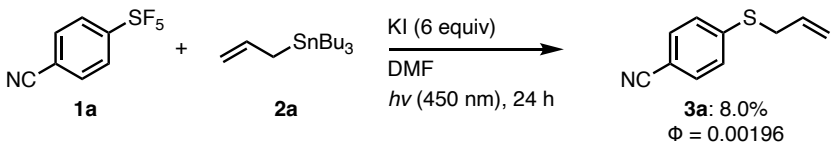

The reaction was performed according to Procedure I to give **3a** (1.4 mg, 0.0080 mmol) in 8.0% yield.

The quantum yield (Φ) was calculated using:

$$\Phi = \frac{mol\ \mathbf{3a}}{I \cdot t \cdot (1 - 10^{-A})}$$

[I: photon flux of blue LED (7.55×10^{-7} mol•s^{-1}), t: reaction time (86400 s), A: absorbance of reaction mixture at 450 nm (0.0634)]

$$\Phi = \frac{0.1 \times 0.080 \times 10^{-3}}{7.55 \times 10^{-7} \cdot 86400 \cdot (1 - 10^{-0.0634})} = 0.000196$$

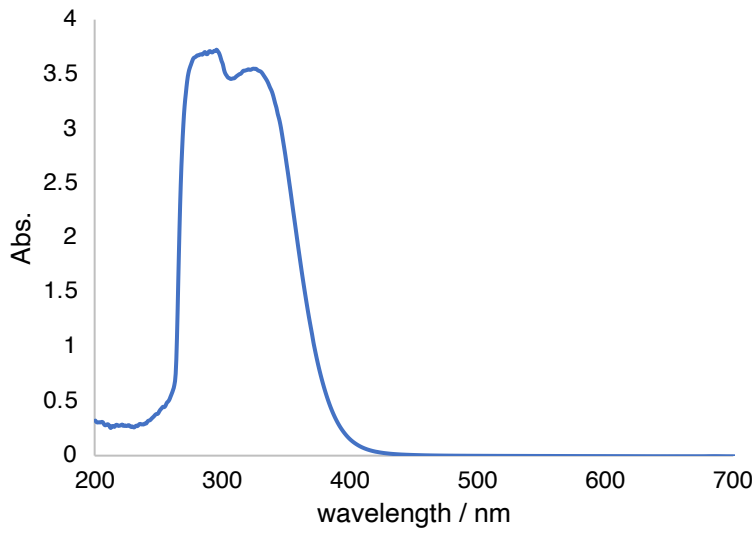

Figure S1. UV–Vis spectrum of reaction mixture.

4-2. UV–Vis spectra

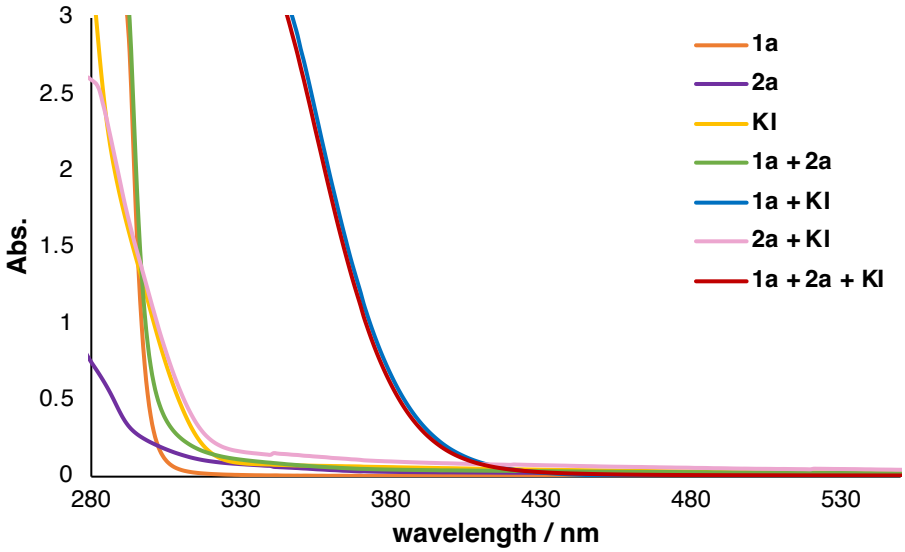

Figure S2. UV–Vis spectra.

In quartz cell (l = 1 cm), **3a** (22.9 mg, 0.01 mmol), **2a** (93.0 μL, 0.3 mmol) and KI (99.6 mg, 0.6 mmol) was dissolved in DMF (3 mL). UV–Vis spectra were measured by V-670 UV–VIS–NIR spectrometer (JASCO Co., Ltd.).

4-3. Emission spectra and Stern-Volmer plot

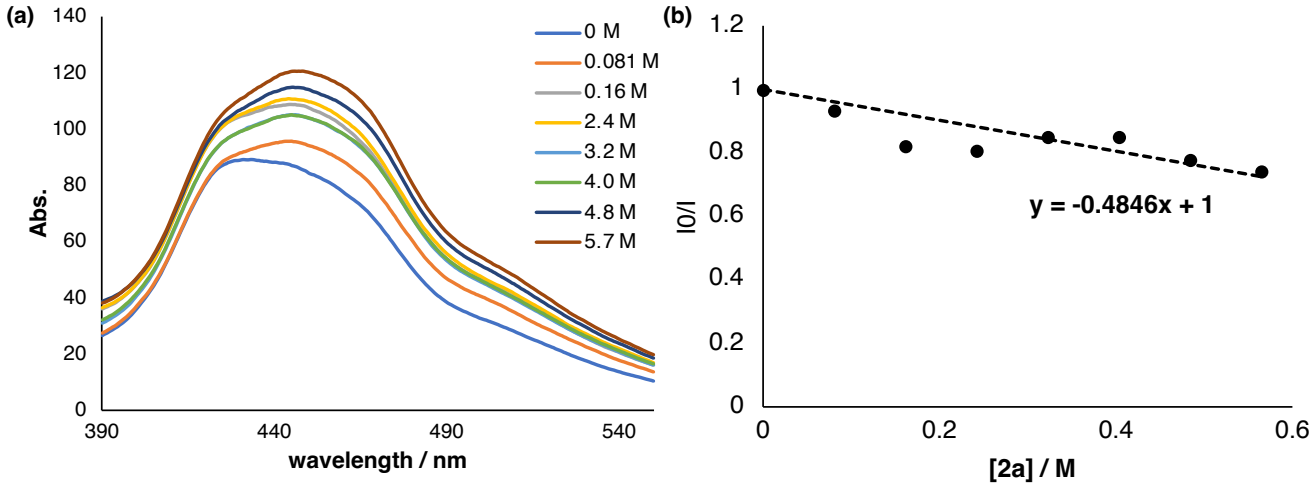

Figure S3. Fluorescence quenching experiments of 1a-LiI. (a) Fluorescence spectra of 1a-KI. (b) Stern-Volmer quenching experiment of 1a-KI

In quartz cell (*l* = 1 cm), various ratio of **2a** was added to DMF (2 mL) solution of **1a** (22.9 mg, 0.10 mmol) and KI (99.6 mg, 0.60 mmol). Then emission spectra were measured by irradiation at 390 nm.

4-4. Cyclic Voltammetry

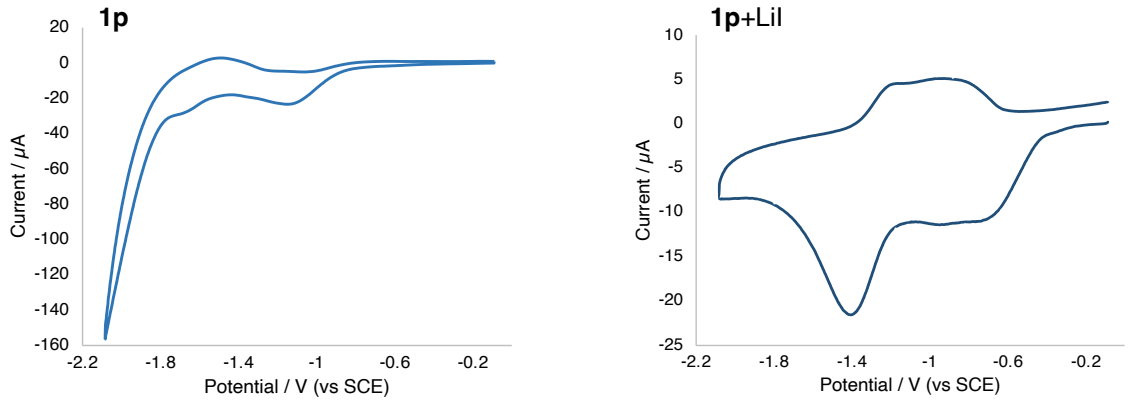

Figure S4. Cyclic voltammetry of 3a

All voltammograms were measured by IUPAC convention at room temperature using $Ag/AgNO_3$ reference electrode, a platinum (Pt) counter and working electrode (polishing 3 times by 1 µm diamond and 0.05 µm alumina). The conditions of the experiments were as follows: a CH_3CN (degassed by nitrogen bubbling) solution of 100 mM tetrabutylammonium hexafluorophosphate (Bu_4NPF_6), initial potential at 0 V, switching potential at 1.0–1.5 V, direction of initial scan to anodic sweep (oxidative), and a scan rate of 50 mV/s. The potentials of **2b** with **1a** and **2b** with **1a** were taken at half-height of the peak ($E_{p/2}$) since the reduction were non-reversible.

In order to convert the potentials from $Ag/AgNO_3$ to Fc/Fc^+ reference, ferrocene was measured under the above conditions in a CH_3CN solution, and –0.44 V was subtracted from the measured values. To convert the potentials from Fc/Fc^+ to SCE reference, +0.38 V was added from the values according to the literature.[S3]

4-5. Detection of iodide

4-5-1. Iodine-starch reaction

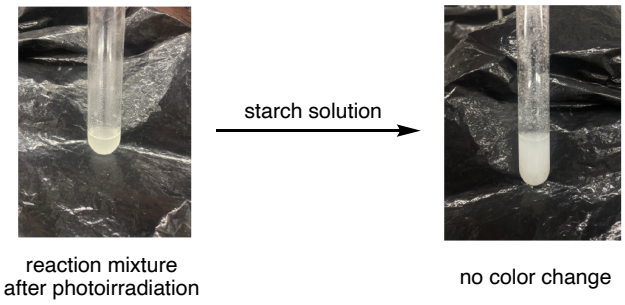

Figure S5. Iodine-starch reaction of reaction mixture

4-5-2. ^{127}I NMR and UV–Vis spectra

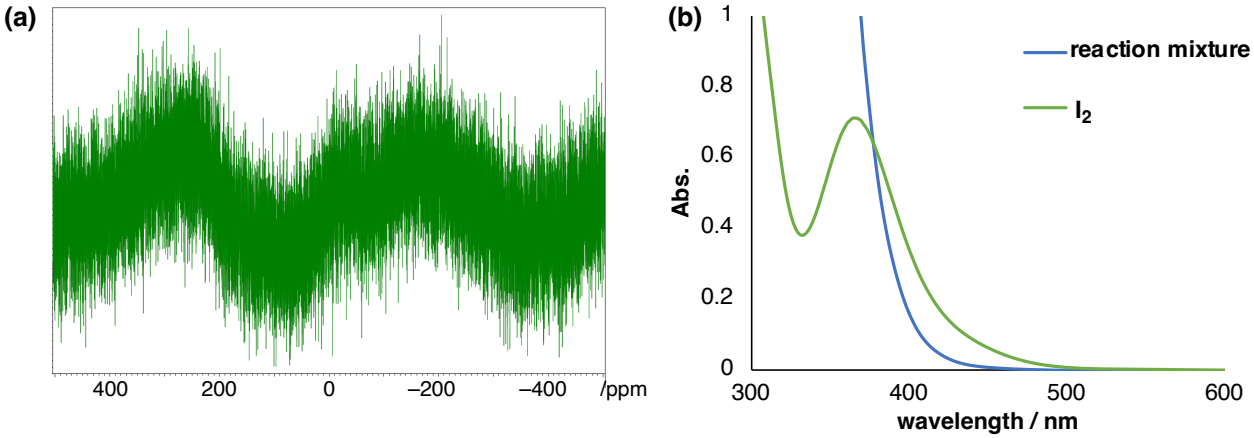

Figure S6. (a) ^{127}I NMR of the reaction mixture after photoirradiation. (b) UV–Vis spectra of the reaction mixture after photoirradiation.

According to these experiments, iodine was not generated in the reaction.

4-6. Determination of the Sn residue after reaction

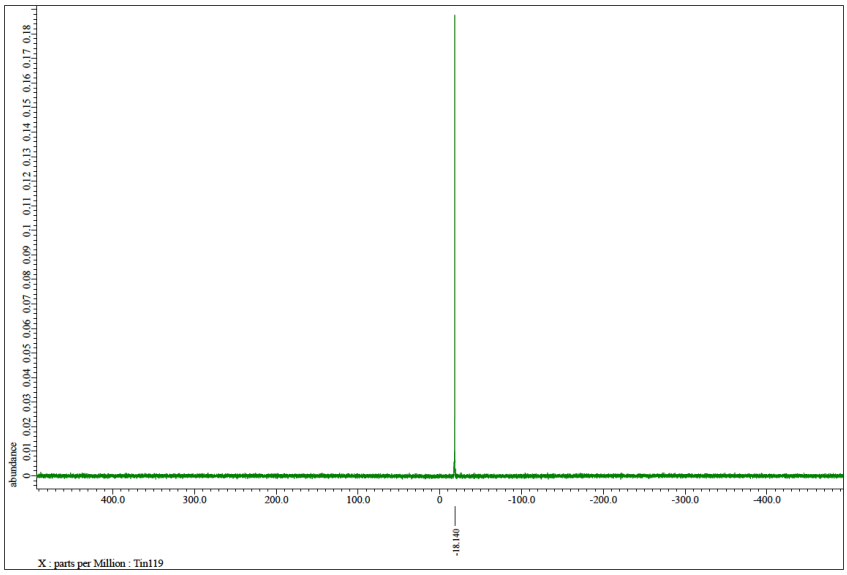

Figure S7. ^{119}Sn NMR of the reaction mixture after light irradiation.

Only unreacted **2a** was observed by ^{119}Sn NMR (–18 ppm, Figure S7). According to ^{119}Sn NMR, Sn residue was determined to be Bu_3SnF as precipitate of reaction mixture. Other plausible species (Bu_3Sn-$SnBu_3$, Bu_3SnI) should be dissolved in DMF and observed by ^{119}Sn NMR.

4-7. DFT calculation

All calculations were performed with Gaussian 16 program using M062x method with basis set of SDD for I and 6-31G(d,p) for other atoms.[S4]

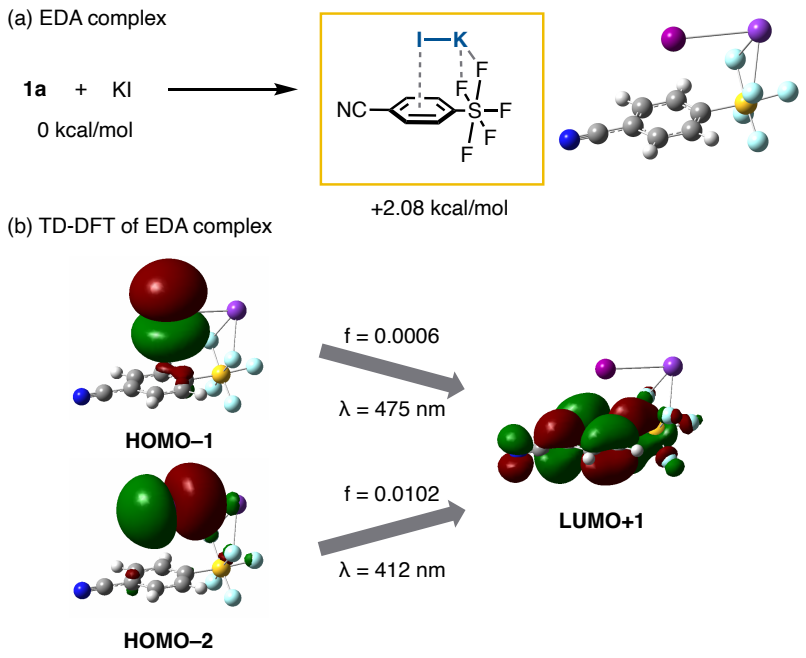

Figure S8. DFT calculation of the EDA complex.

Calculating the conformation and Gibbs free energy of the EDA complex revealed a converged structure of **1a** and potassium iodide, the energy of which was 2.08 kcal/mol. Although formation reaction is endergonic, the Gibbs free energy was sufficiently low to form the EDA complex. In this converged structure, iodide interacted with the aromatic moiety of **1a**, and the potassium cation interacted with two fluorine atoms of the pentafluorosulfanyl group. Therefore, the formation of the EDA complex of acceptor **1a** and donor iodide was verified.

We also investigated the excitation of the EDA complex through TD-DFT calculations. The absorption wavelength, derived from the electronic transition from the iodide into the aromatic moiety of **1a**, was consistent with the observed UV–vis spectra (Figure 3a). Thus, we confirmed that the single-electron transfer occurred during EDA complex excitation.

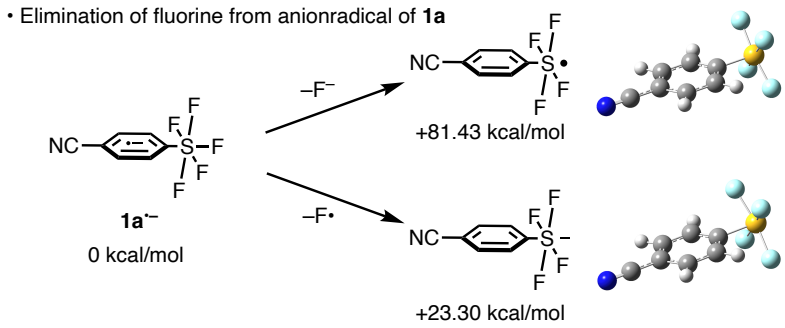

Figure S9. DFT calculation of the energy of tetrafluorosulfanyl radical or anion.

Radical anion species **1a**$^{\bullet-}$ was generated through the single-electron reduction of **1a**. We calculated two pathways: the elimination of fluoride and the elimination of fluorine radical. DFT calculations indicated that the latter was favorable (ΔΔG = 58.1 kcal/mol).

• Comparing the reduction energy of fluorosulfanyl compounds

$$ArSF_n \xrightarrow{+\,e^-} \overset{-\bullet}{ArSF_n}$$

n	ΔΔG/ kcal•mol^{-1}
5	0
3	–8.86
1	–2.89

Figure S10. Reduction energy of fluorosulfanyl compounds.

We calculated the single-electron reduction of $ArSF_5$ (**1a**), $ArSF_3$, and ArSF, and from the ΔG values, confirmed that $ArSF_5$ reduction required the highest energy. We supposed that the generated $ArSF_3$ and ArSF underwent immediate reduction to give thiyl radical (ArS•), which reacted with allyl radicals to furnish sulfides.

Table S2. Sum of electronic and thermal free energies

	G (hartree)	G (kcal/mol)
1a	-1220.7777	-766050.20
KI	-611.35055	-383628.58
1a-KI (EDA)	-1832.1250	-1149676.80
$1a^{\bullet-}$	-1220.8082	-766069.36
$ArSF4^{\bullet}$	-1120.9409	-703401.65
F^{-}	-99.737509	-62586.284
$ArSF4^{-}$	-1121.0738	-703485.02
$F^{\bullet}$	-99.697268	-62561.033
ArSF3	-1021.1979	-640811.92
$ArSF3^{\bullet-}$	-1021.2426	-640839.94
ArSF	-821.62968	-515580.84
$ArSF^{\bullet-}$	-821.66482	-515602.89

TD-DFT calculation of 1a-KI

Table S3. Result of TD-DFT.

Excitation energies and oscillator strengths:

```
Excited State   1:      Singlet-A      0.1580 eV 7846.34 nm   f=0.0000   <S**2>=0.000
     69 -> 71           0.69902
This state for optimization and/or second-order correction.
Total Energy, E(TD-HF/TD-DFT) =    -1832.12294098
Copying the excited state density for this state as the 1-particle RhoCI density.

Excited State   2:      Singlet-A      0.2397 eV 5172.29 nm   f=0.0000   <S**2>=0.000
     70 -> 71           0.70442

Excited State   3:      Singlet-A      0.6461 eV 1918.96 nm   f=0.0112   <S**2>=0.000
     68 -> 71           0.70309

Excited State   4:      Singlet-A      2.6119 eV   474.68 nm   f=0.0006   <S**2>=0.000
     69 -> 72           0.68801
     69 -> 73           0.13896

Excited State   5:      Singlet-A      2.6937 eV   460.28 nm   f=0.0000   <S**2>=0.000
     70 -> 72           0.69049
     70 -> 73           0.13324

Excited State   6:      Singlet-A      3.0075 eV   412.25 nm   f=0.0106   <S**2>=0.000
     68 -> 72           0.69399
     68 -> 73           0.12305
```

No.	orbital	picture	energy/ eV	No.	orbital	picture	energy/ eV
70	**HOMO**	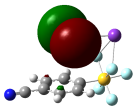	–5.93	73	**LUMO+2**	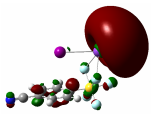	–1.22
69	**HOMO–1**	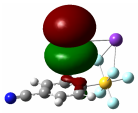	–5.94	72	**LUMO+1**	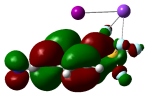	–1.36
68	**HOMO–2**	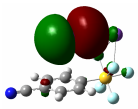	–6.25	71	**LUMO**	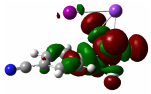	–3.89
67	**HOMO–3**	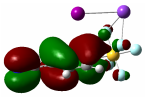	–9.39				

Cartesian Coordinates

1a

Charge = 0 Multiplicity = 1

Center Number	Atomic Number	Atomic Type	Coordinates (Angstroms) X	Y	Z
1	6	0	2.116916	1.208126	-0.000284
2	6	0	0.721756	1.208038	-0.000783
3	6	0	0.024294	0.000243	-0.000289
4	6	0	0.722024	-1.208223	-0.000494
5	6	0	2.116849	-1.208057	-0.000474
6	6	0	2.814374	0.000194	0.000028
7	1	0	2.666615	2.160478	-0.000223
8	1	0	0.172188	2.160517	-0.000251
9	1	0	0.171884	-2.160400	-0.000164
10	1	0	2.667032	-2.160304	-0.000643
11	6	0	4.354374	0.000034	0.000327
12	7	0	5.500974	-0.000082	0.000551
13	16	0	-1.755706	0.000002	0.000100
14	9	0	-1.755308	-1.124235	1.124463
15	9	0	-1.755613	1.124364	1.124337
16	9	0	-1.756104	1.124239	-1.124262
17	9	0	-1.755799	-1.124361	-1.124137
18	9	0	-3.345706	-0.000214	0.000448

KI

Charge = 0 Multiplicity = 1

Center Number	Atomic Number	Atomic Type	Coordinates (Angstroms) X	Y	Z
1	53	0	0.000000	0.000000	0.886667
2	19	0	0.000000	0.000000	-2.473333

1a-KI

Charge = 0 Multiplicity = 1

Center Number	Atomic Number	Atomic Type	Coordinates (Angstroms) X	Y	Z
1	6	0	-2.259630	-0.933912	1.224899
2	6	0	-0.886056	-0.732145	1.227492
3	6	0	-0.224907	-0.670417	0.006518
4	6	0	-0.879056	-0.801776	-1.212729
5	6	0	-2.252654	-1.003288	-1.206504
6	6	0	-2.938908	-1.068828	0.010101
7	1	0	-2.807431	-0.987319	2.158432
8	1	0	-0.348816	-0.626197	2.162118
9	1	0	-0.336455	-0.749211	-2.148783
10	1	0	-2.795107	-1.109931	-2.138596
11	6	0	-4.363575	-1.277963	0.011977
12	7	0	-5.507393	-1.445872	0.013523
13	16	0	1.548574	-0.410082	0.004226
14	9	0	1.507673	0.689168	-1.157807
15	9	0	1.501103	0.753522	1.101536
16	9	0	1.828229	-1.474296	1.165923
17	9	0	1.834793	-1.538560	-1.093467
18	9	0	3.205195	-0.166831	0.002032
19	19	0	5.666645	0.194822	-0.001330
20	53	0	-1.767323	1.339932	-0.013295

$1a^{\bullet-}$

Charge = –1 Multiplicity = 2

Center Number	Atomic Number	Atomic Type	Coordinates (Angstroms) X	Y	Z
1	6	0	-2.146769	1.215091	-0.000043
2	6	0	-0.758349	1.216803	-0.000001
3	6	0	-0.087937	0.000019	0.000001
4	6	0	-0.758330	-1.216776	-0.000040
5	6	0	-2.146750	-1.215092	-0.000082
6	6	0	-2.838102	-0.000007	-0.000085
7	1	0	-2.697223	2.148692	-0.000044
8	1	0	-0.207979	2.149578	0.000035
9	1	0	-0.207944	-2.149543	-0.000034
10	1	0	-2.697188	-2.148702	-0.000113
11	6	0	-4.278436	-0.000021	-0.000131
12	7	0	-5.435004	-0.000014	-0.000167
13	16	0	1.717759	0.000030	0.000068
14	9	0	1.787902	-1.137492	-1.133802
15	9	0	1.787932	1.137555	-1.133812
16	9	0	1.787860	1.137542	1.133974
17	9	0	1.787830	-1.137571	1.133872
18	9	0	3.343949	-0.000089	0.000052

$ArSF_4^{\bullet}$

Charge = 0 Multiplicity = 2

Center Number	Atomic Number	Atomic Type	Coordinates (Angstroms) X	Y	Z
1	6	0	1.857241	1.214708	-0.000004
2	6	0	0.468706	1.215810	-0.000012
3	6	0	-0.203723	0.000016	-0.000005
4	6	0	0.468737	-1.215797	-0.000007
5	6	0	1.857242	-1.214671	-0.000009
6	6	0	2.549119	0.000038	0.000002
7	1	0	2.407014	2.148773	0.000000
8	1	0	-0.081236	2.148777	-0.000008
9	1	0	-0.081224	-2.148752	-0.000003
10	1	0	2.407074	-2.148704	-0.000005
11	6	0	3.989371	0.000009	0.000005
12	7	0	5.146008	-0.000036	0.000009
13	16	0	-2.011370	-0.000009	0.000001

14	9	0	-2.066977	-1.136941	1.133551
15	9	0	-2.067013	1.136893	1.133578
16	9	0	-2.067019	1.136920	-1.133547
17	9	0	-2.066979	-1.136914	-1.133574

$ArSF_4^-$

Charge = –1 Multiplicity = 1

Center Number	Atomic Number	Atomic Type	Coordinates (Angstroms) X	Y	Z
1	6	0	-1.857917	1.216166	-0.000004
2	6	0	-0.469878	1.218336	-0.000004
3	6	0	0.196470	0.000001	0.000000
4	6	0	-0.469880	-1.218334	0.000004
5	6	0	-1.857917	-1.216163	0.000003
6	6	0	-2.548183	0.000003	0.000000
7	1	0	-2.409506	2.149023	-0.000007
8	1	0	0.087456	2.146857	-0.000007
9	1	0	0.087455	-2.146855	0.000007
10	1	0	-2.409509	-2.149018	0.000006
11	6	0	-3.988578	-0.000000	-0.000001
12	7	0	-5.145179	-0.000002	-0.000001
13	16	0	1.980011	-0.000001	0.000000
14	9	0	2.082096	-1.170960	-1.160019
15	9	0	2.082098	1.170947	-1.160030
16	9	0	2.082098	1.170959	1.160020
17	9	0	2.082096	-1.170948	1.160031

$ArSF_3$

Charge = 0 Multiplicity = 1

Center Number	Atomic Number	Atomic Type	Coordinates (Angstroms) X	Y	Z
1	6	0	-2.485167	0.000158	-0.000052
2	6	0	-1.787452	-1.208008	-0.000488
3	6	0	-0.392740	-1.208062	-0.000062
4	6	0	0.304898	0.000457	-0.000399
5	6	0	-0.392717	1.208294	-0.000442
6	6	0	-1.787855	1.208175	0.000128
7	1	0	-2.337492	-2.160214	0.000147
8	1	0	0.157276	-2.160311	0.000228
9	1	0	0.156815	2.160916	-0.000715
10	1	0	-2.337605	2.160490	0.000292
11	6	0	-4.025167	-0.000089	0.000108
12	7	0	-5.171767	-0.000273	0.000227
13	16	0	2.084897	-0.000017	0.000049
14	9	0	2.614511	-0.033102	1.498887
15	9	0	2.614752	-1.281601	-0.777701
16	9	0	2.615429	1.314230	-0.720639

$ArSF_3^{\bullet-}$

Charge = –1 Multiplicity = 2

Center Number	Atomic Number	Atomic Type	Coordinates (Angstroms) X	Y	Z
1	6	0	-2.485167	0.000158	-0.000052
2	6	0	-1.787452	-1.208008	-0.000488
3	6	0	-0.392740	-1.208062	-0.000062
4	6	0	0.304898	0.000457	-0.000399
5	6	0	-0.392717	1.208294	-0.000442
6	6	0	-1.787855	1.208175	0.000128
7	1	0	-2.337492	-2.160214	0.000147
8	1	0	0.157276	-2.160311	0.000228
9	1	0	0.156815	2.160916	-0.000715
10	1	0	-2.337605	2.160490	0.000292
11	6	0	-4.025167	-0.000089	0.000108
12	7	0	-5.171767	-0.000273	0.000227
13	16	0	2.084897	-0.000017	0.000049
14	9	0	2.614511	-0.033102	1.498887
15	9	0	2.614752	-1.281601	-0.777701
16	9	0	2.615429	1.314230	-0.720639

ArSF

Charge = 0 Multiplicity = 1

Center Number	Atomic Number	Atomic Type	Coordinates (Angstroms) X	Y	Z
1	6	0	-1.877118	-0.011756	0.001536
2	6	0	-1.246689	1.231214	0.099694
3	6	0	0.136340	1.311292	0.005154
4	6	0	0.870209	0.146851	-0.213064
5	6	0	0.250624	-1.096528	-0.325264
6	6	0	-1.129234	-1.175465	-0.203181
7	1	0	-1.838276	2.125080	0.259991
8	1	0	0.639333	2.262646	0.111068
9	1	0	0.842180	-1.982699	-0.509010
10	1	0	-1.631741	-2.133323	-0.272700
11	6	0	-3.310922	-0.095187	0.111057
12	7	0	-4.462327	-0.162002	0.198467
13	16	0	2.659707	0.272054	-0.359079
14	9	0	3.167802	-0.594788	0.879006

$ArSF^{\bullet-}$

Charge = –1 Multiplicity = 2

Center Number	Atomic Number	Atomic Type	Coordinates (Angstroms) X	Y	Z
1	6	0	-1.877118	-0.011756	0.001536
2	6	0	-1.246689	1.231214	0.099694
3	6	0	0.136340	1.311292	0.005154
4	6	0	0.870209	0.146851	-0.213064
5	6	0	0.250624	-1.096528	-0.325264
6	6	0	-1.129234	-1.175465	-0.203181

7	1	0	-1.838276	2.125080	0.259991
8	1	0	0.639333	2.262646	0.111068
9	1	0	0.842180	-1.982699	-0.509010
10	1	0	-1.631741	-2.133323	-0.272700
11	6	0	-3.310922	-0.095187	0.111057
12	7	0	-4.462327	-0.162002	0.198467
13	16	0	2.659707	0.272054	-0.359079
14	9	0	3.167802	-0.594788	0.879006

---

5. References

S1) Y. Wang, L. Deng, X. Wang, Z. Wu, Y. Wang, Y. Pan, Y. *ACS Catal.*, 2019, **9**, 1630–1634.

S2) T. Uchikura, N. Kamiyama, T. Mouri, T. Akiyama, *ACS Catal.*, 2022, **12**, 5209–5216.

S3) V. V. Pavlishchuk, A. W. Addison, *Inorganica Chim. Acta*, 2000, **298**, 97–102.

S4) Gaussian 16, Revision C.01, M. J. Frisch, G. W. Trucks, H. B. Schlegel, G. E. Scuseria, M. A. Robb, J. R. Cheeseman, G. Scalmani, V. Barone, G. A. Petersson, H. Nakatsuji, X. Li, M. Caricato, A. V. Marenich, J. Bloino, B. G. Janesko, R. Gomperts, B. Mennucci, H. P. Hratchian, J. V. Ortiz, A. F. Izmaylov, J. L. Sonnenberg, D. Williams-Young, F. Ding, F. Lipparini, F. Egidi, J. Goings, B. Peng, A. Petrone, T. Henderson, D. Ranasinghe, V. G. Zakrzewski, J. Gao, N. Rega, G. Zheng, W. Liang, M. Hada, M. Ehara, K. Toyota, R. Fukuda, J. Hasegawa, M. Ishida, T. Nakajima, Y. Honda, O. Kitao, H. Nakai, T. Vreven, K. Throssell, J. A. Montgomery, Jr., J. E. Peralta, F. Ogliaro, M. J. Bearpark, J. J. Heyd, E. N. Brothers, K. N. Kudin, V. N. Staroverov, T. A. Keith, R. Kobayashi, J. Normand, K. Raghavachari, A. P. Rendell, J. C. Burant, S. S. Iyengar, J. Tomasi, M. Cossi, J. M. Millam, M. Klene, C. Adamo, R. Cammi, J. W. Ochterski, R. L. Martin, K. Morokuma, O. Farkas, J. B. Foresman, D. J. and Fox, Gaussian, Inc., Wallingford CT, 2019.

6. NMR spectra

3a

^{1}H NMR (400 MHz, $CDCl_3$)

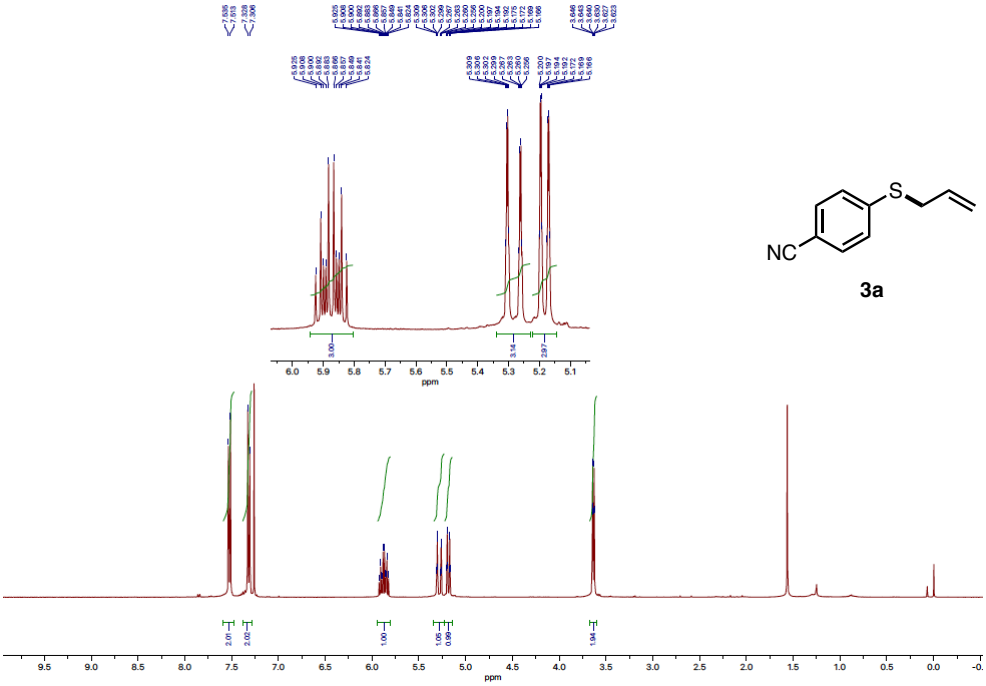

^{13}C{^{1}H} NMR (101 MHz, $CDCl_3$)

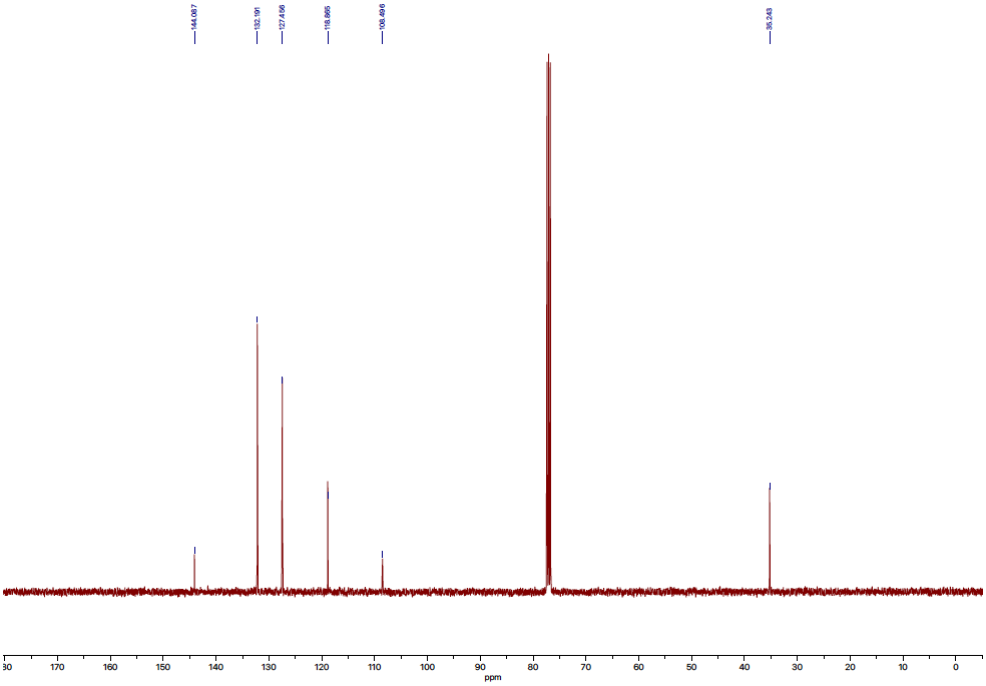

3b

^{1}H NMR (400 MHz, $CDCl_3$)

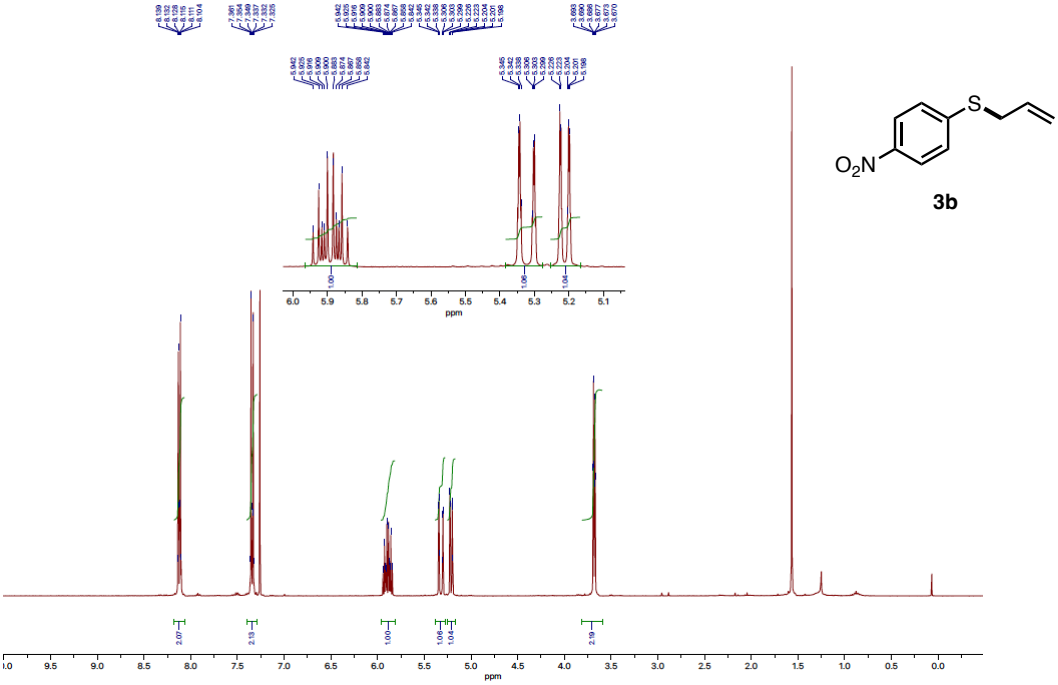

^{13}C{^{1}H} NMR (101 MHz, $CDCl_3$)

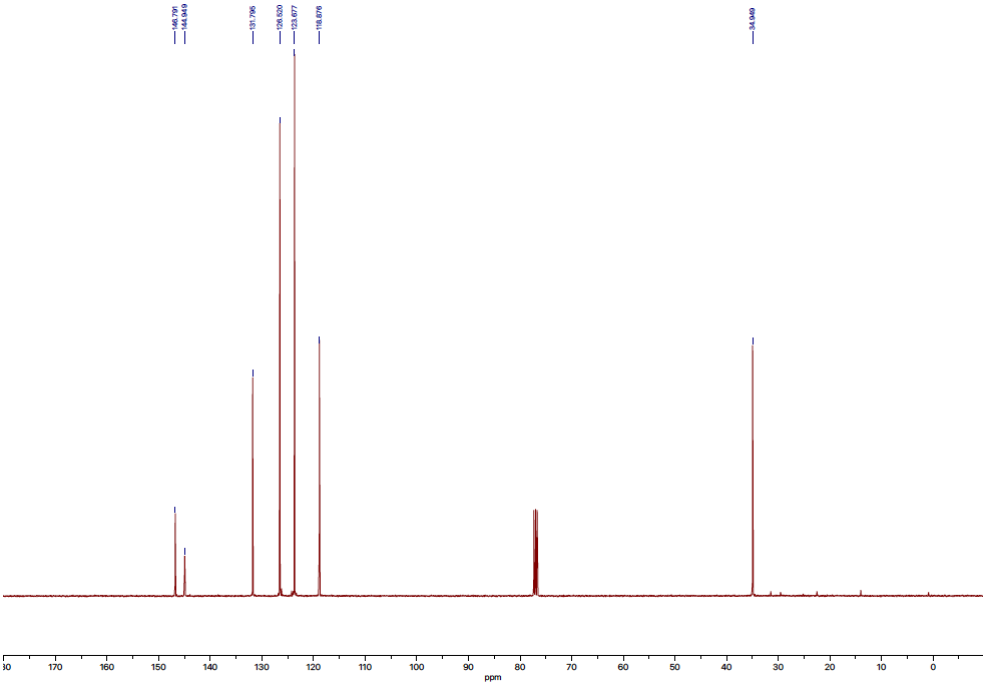

3c

^{1}H NMR (400 MHz, $CDCl_3$)

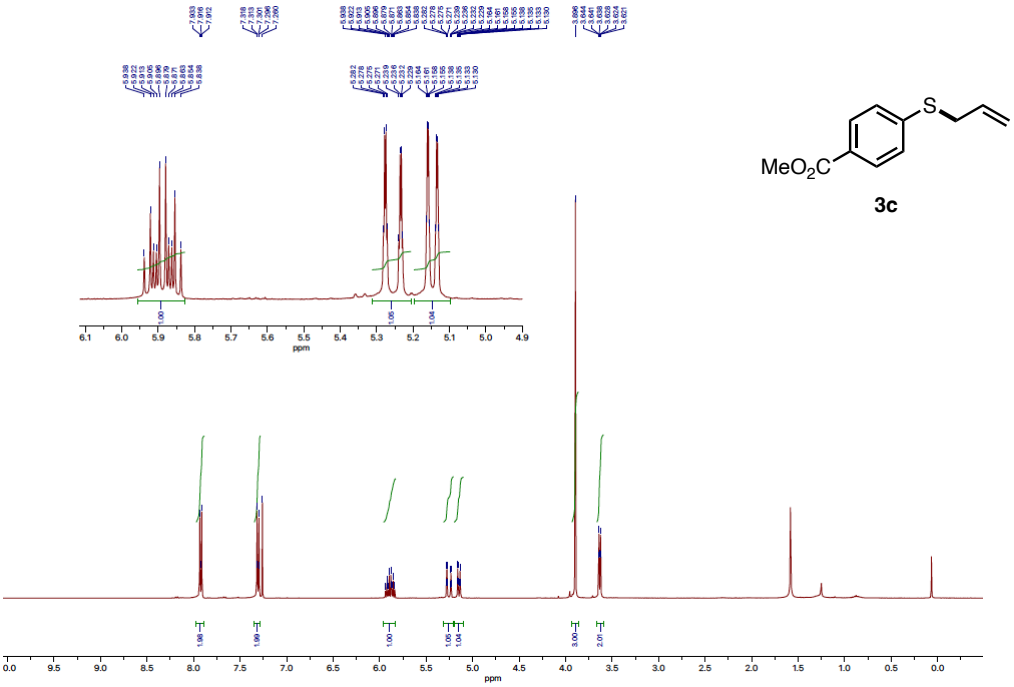

^{13}C{^{1}H} NMR (101 MHz, $CDCl_3$)

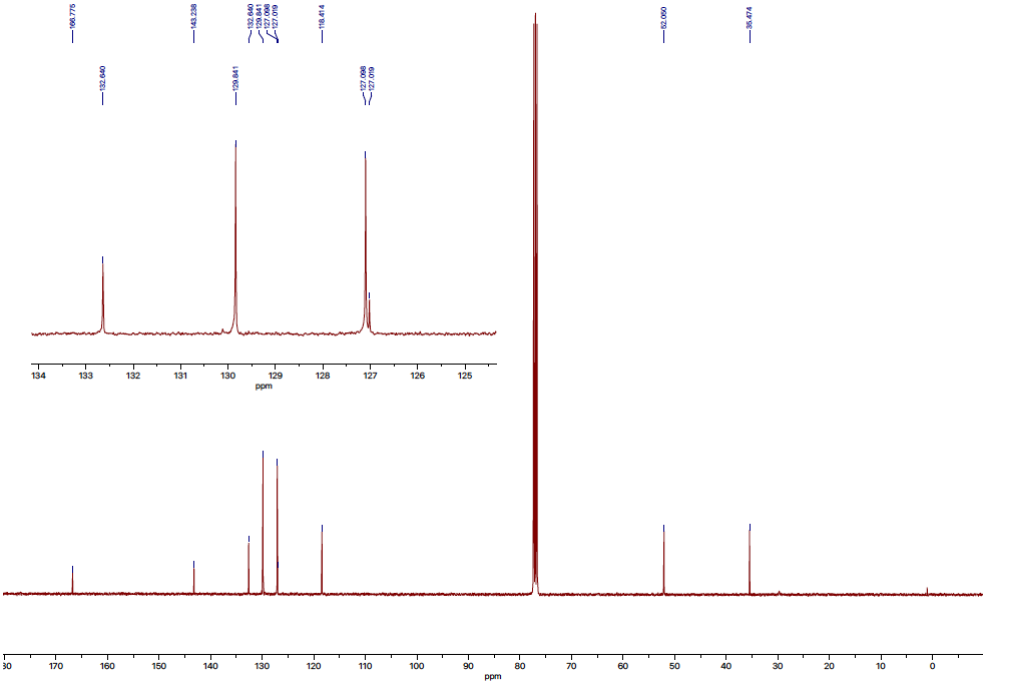

3d

^{1}H NMR (400 MHz, $CDCl_3$)

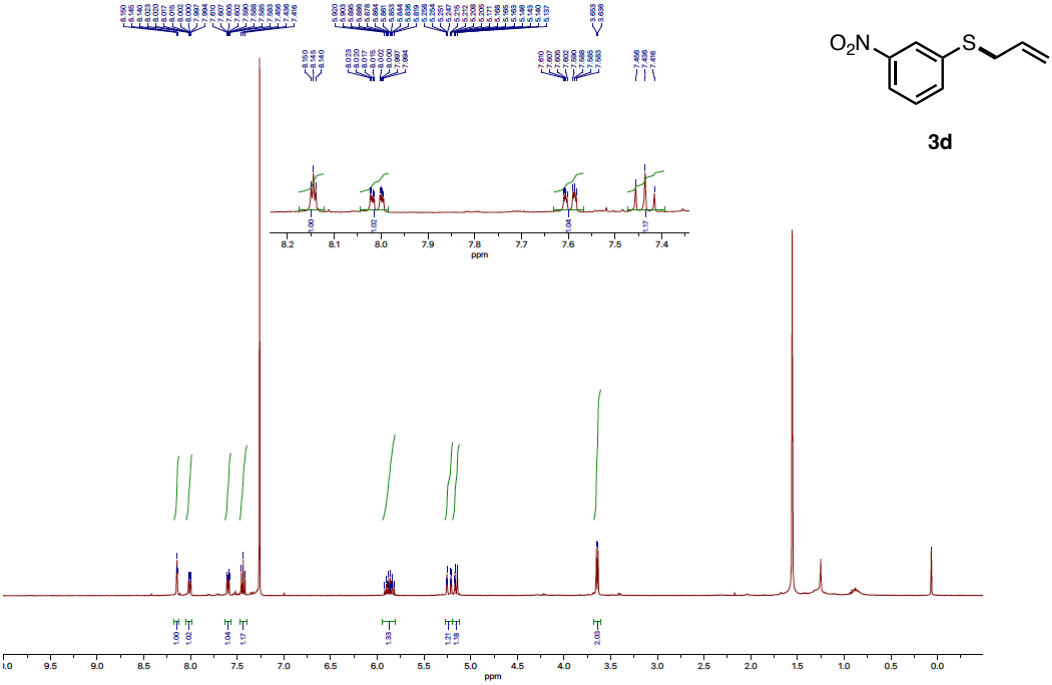

^{13}C{^{1}H} NMR (101 MHz, $CDCl_3$)

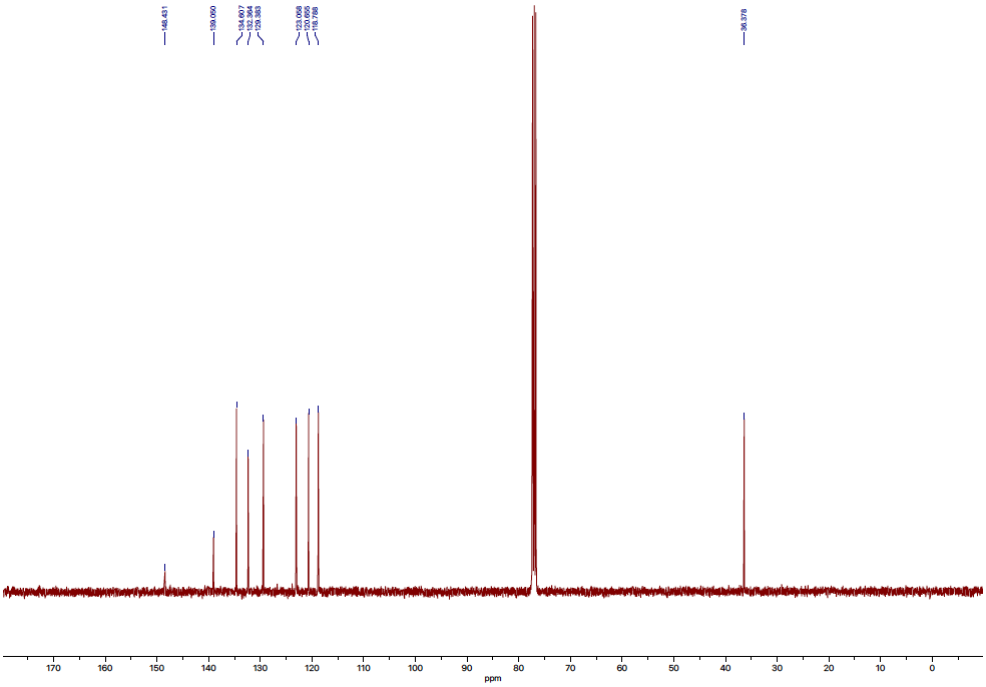

4b

^{1}H NMR (400 MHz, $CDCl_3$)

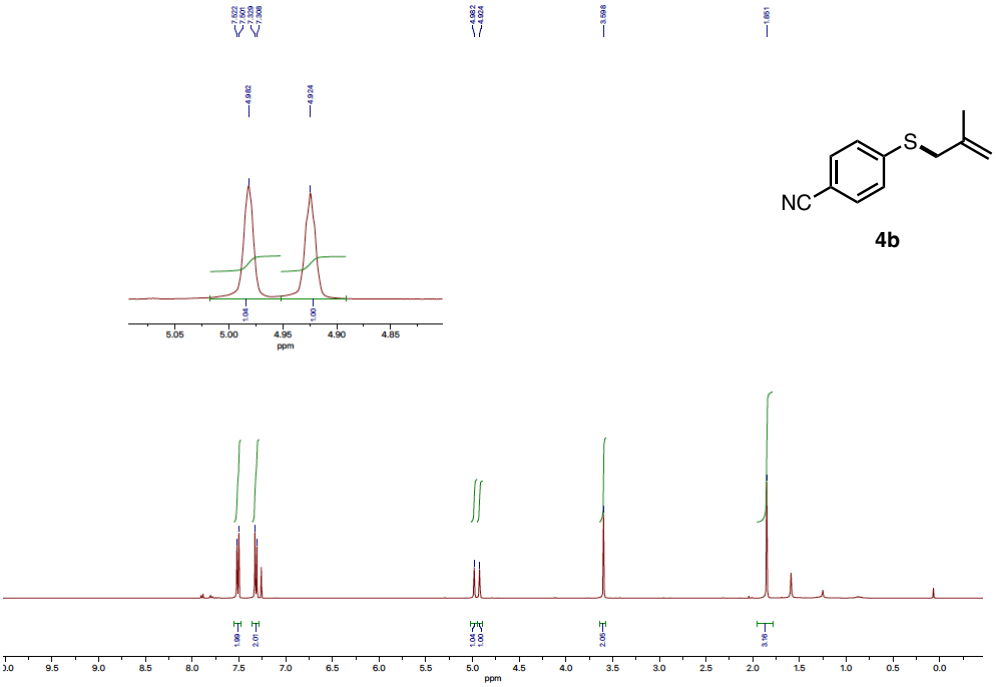

^{13}C{^{1}H} NMR (101 MHz, $CDCl_3$)

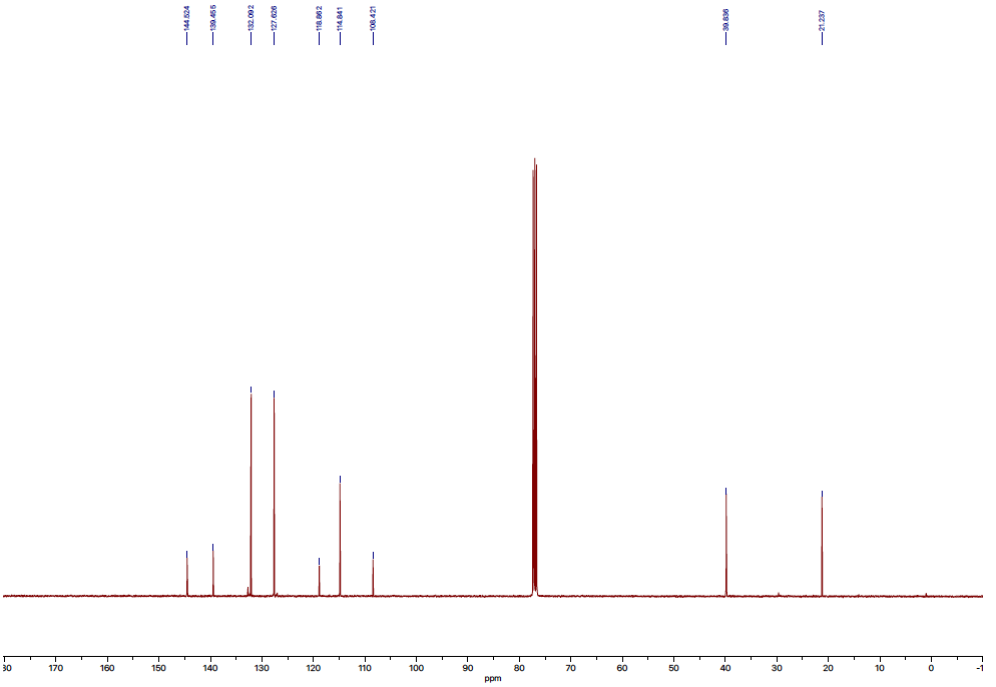

4c

^{1}H NMR (400 MHz, $CDCl_3$)

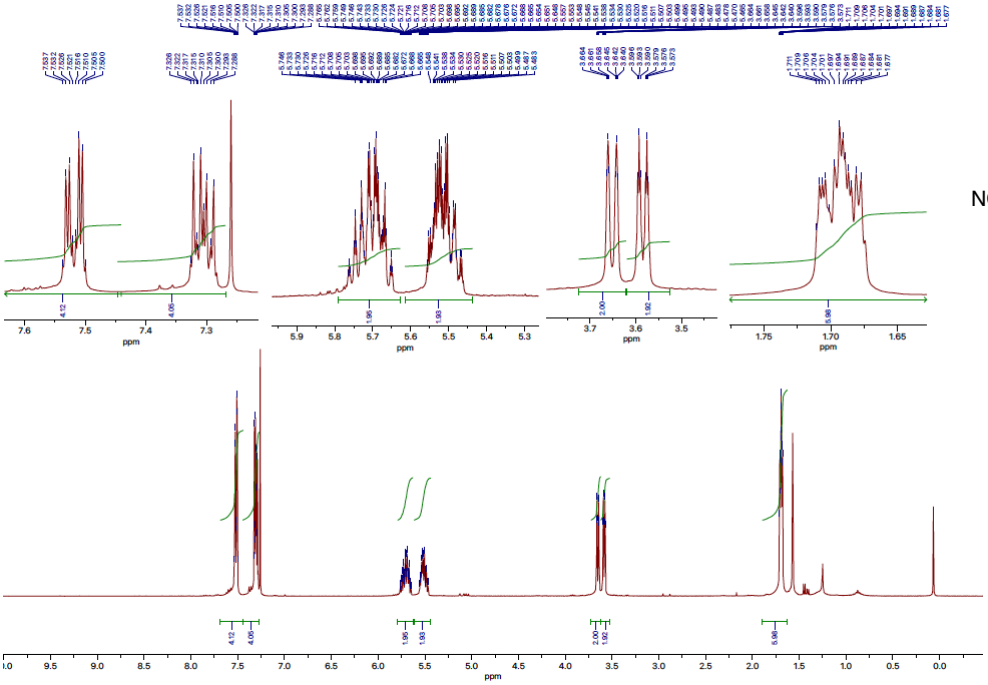

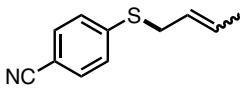

4c

^{13}C{^{1}H} NMR (101 MHz, $CDCl_3$)

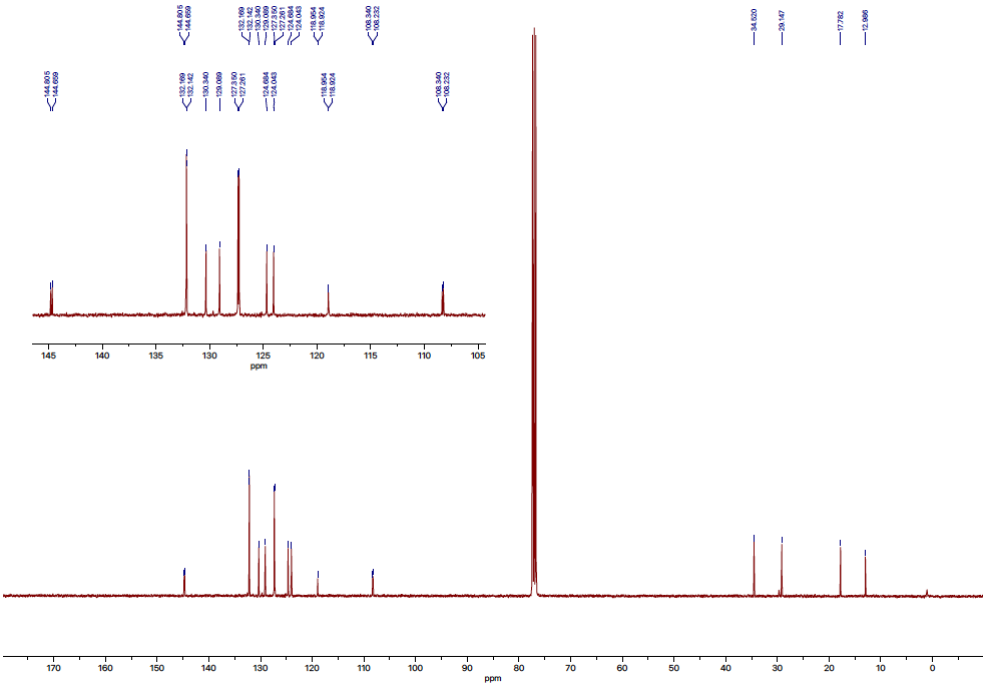

4d

^{1}H NMR (400 MHz, $CDCl_3$)

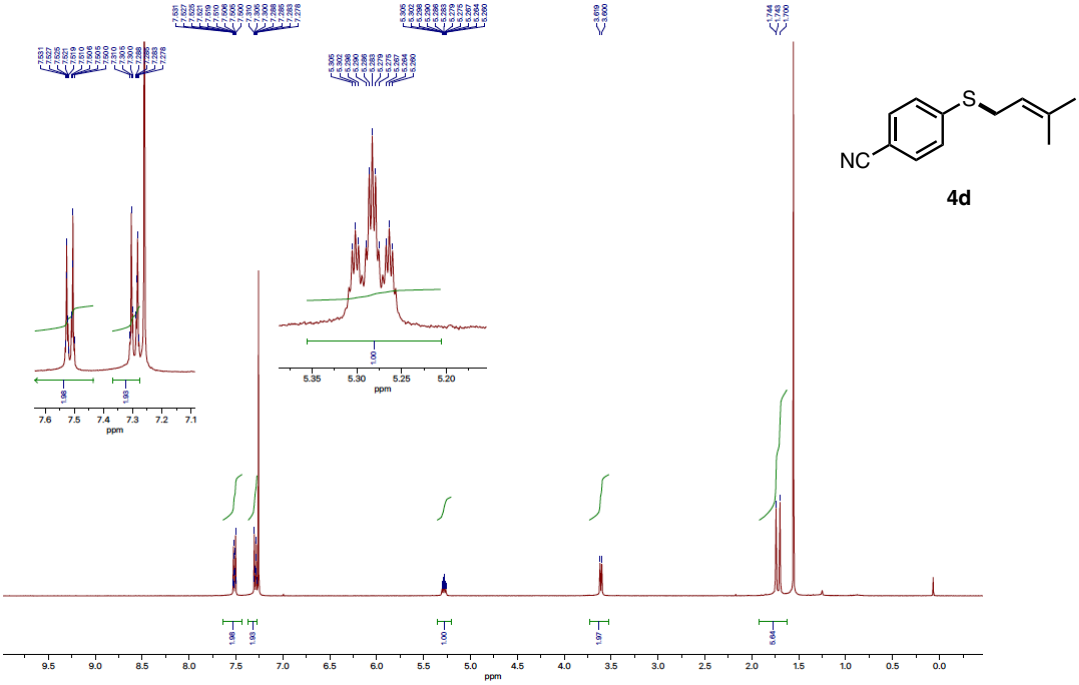

^{13}C{^{1}H} NMR (101 MHz, $CDCl_3$)

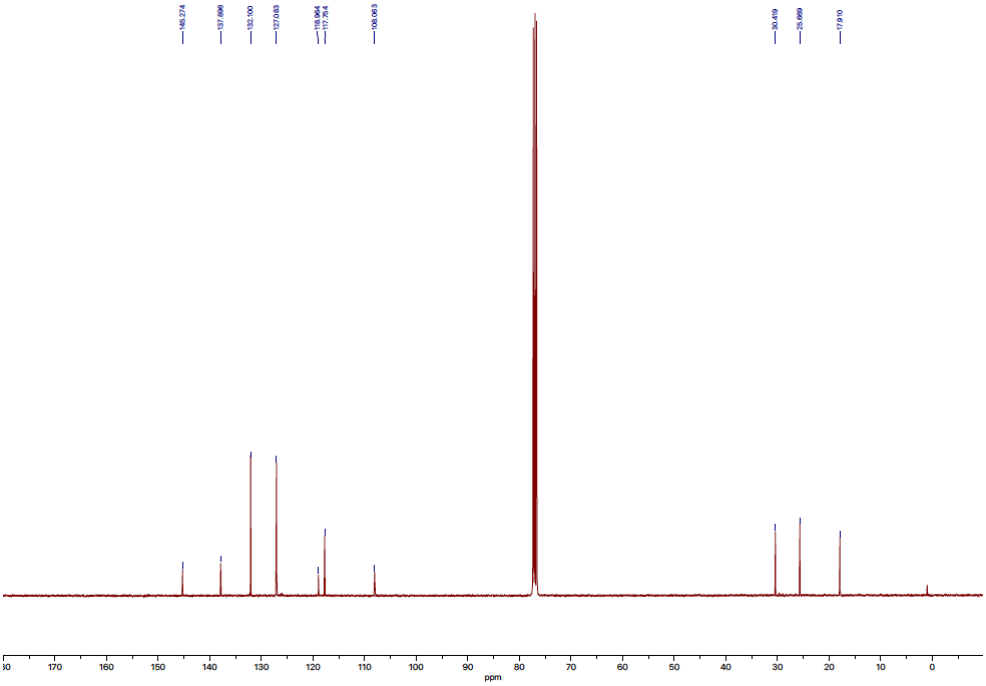

4e

^{1}H NMR (400 MHz, $CDCl_3$)

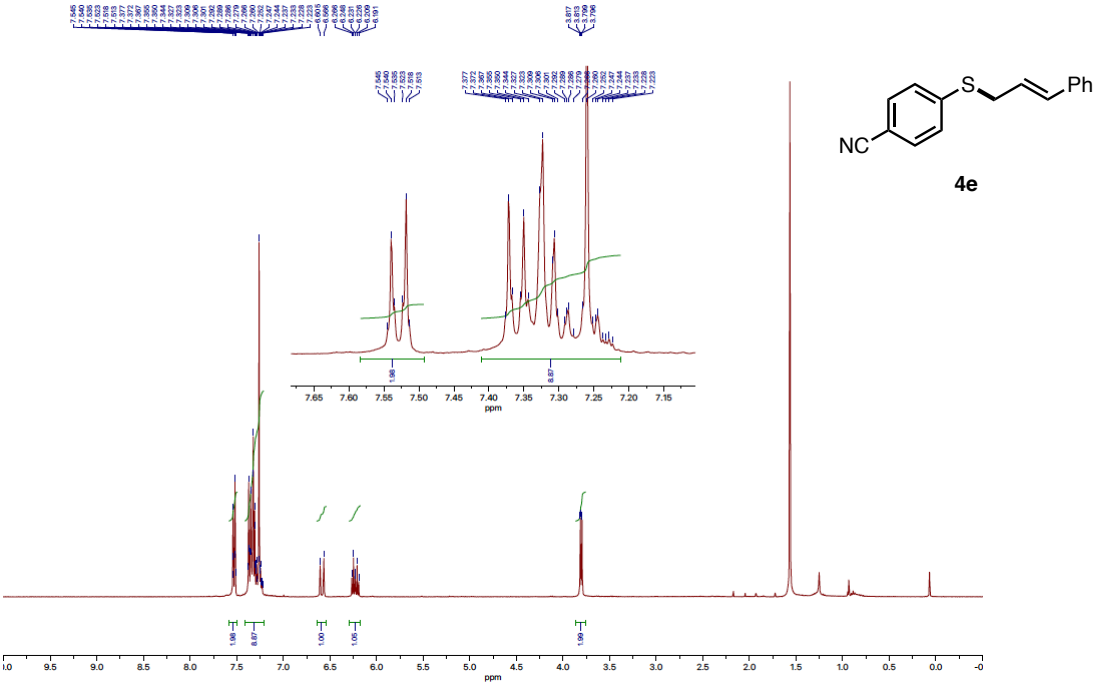

^{13}C{^{1}H} NMR (101 MHz, $CDCl_3$)

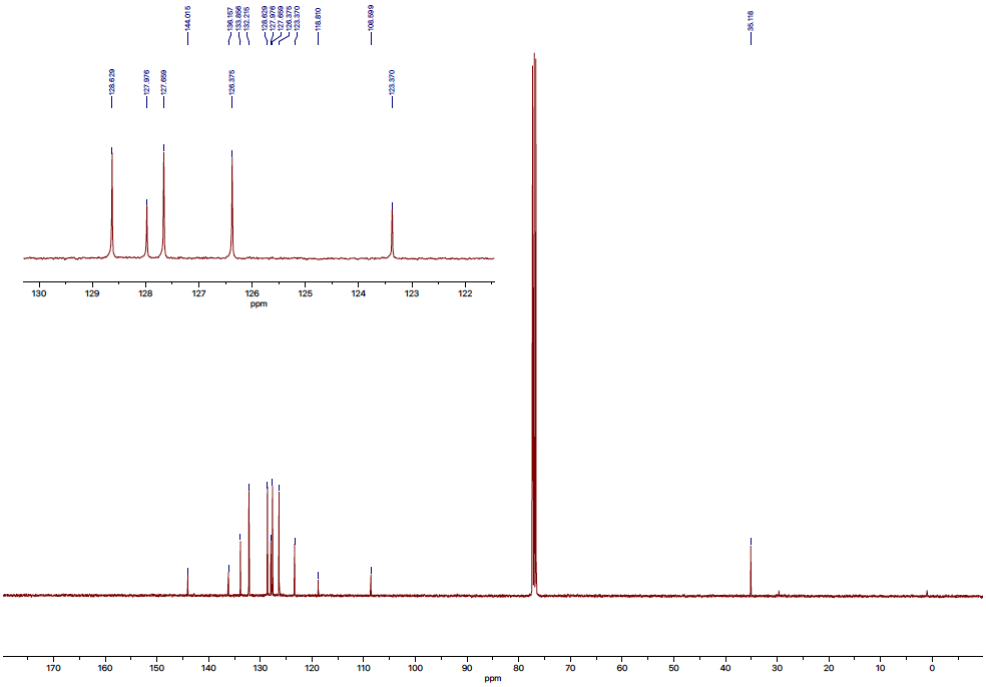

4f

^{1}H NMR (400 MHz, $CDCl_3$)

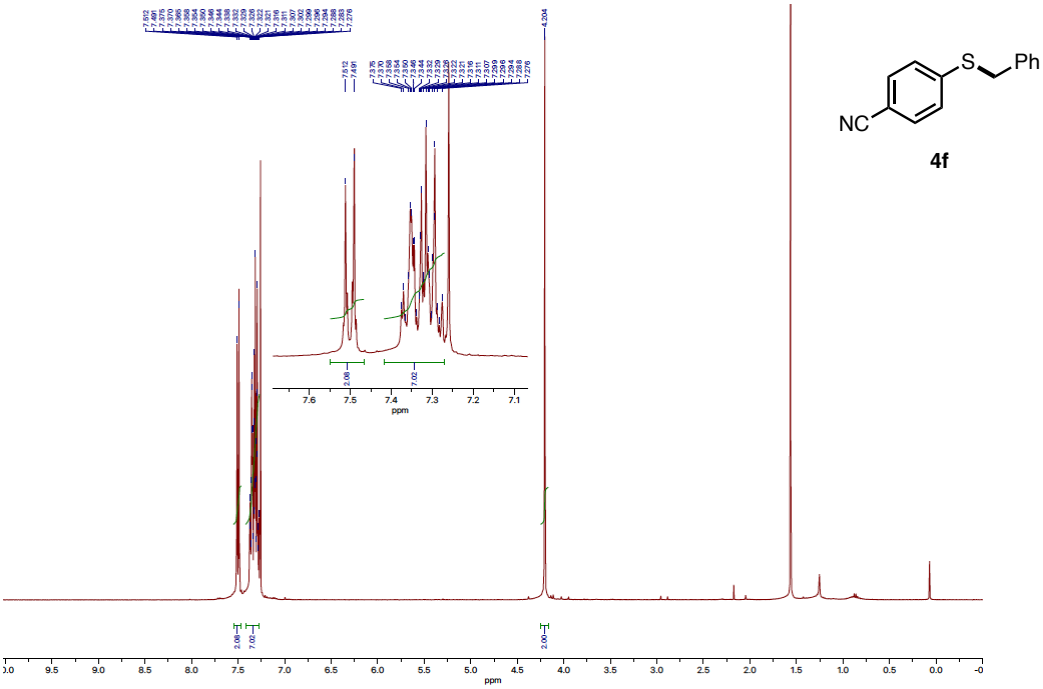

^{13}C{^{1}H} NMR (101 MHz, $CDCl_3$)

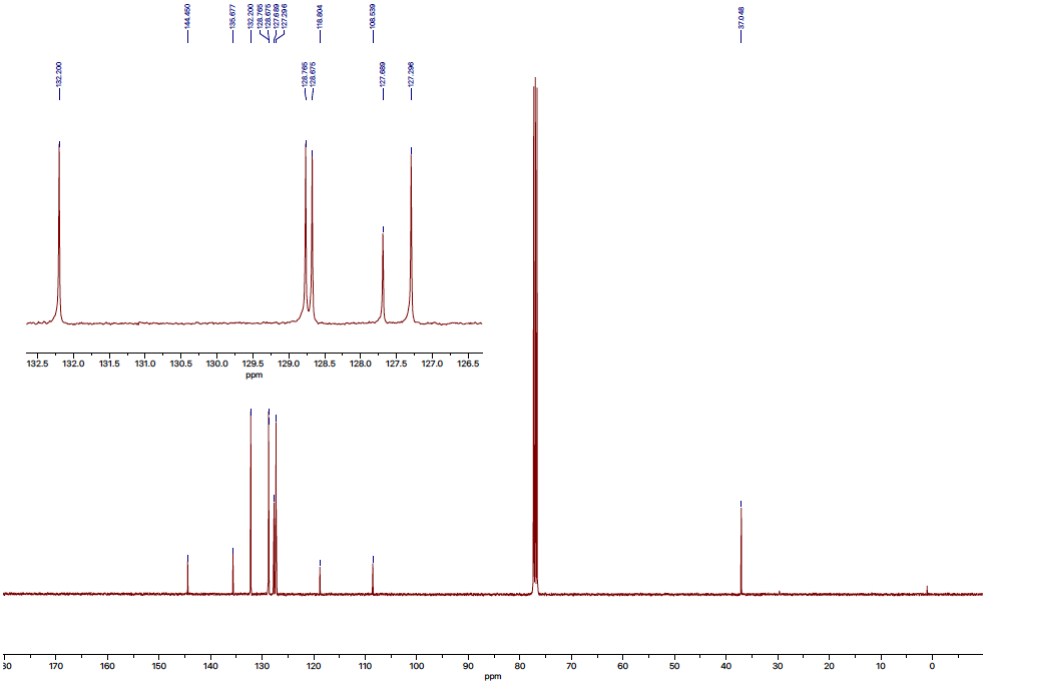

4g

^{1}H NMR (400 MHz, $CDCl_3$)

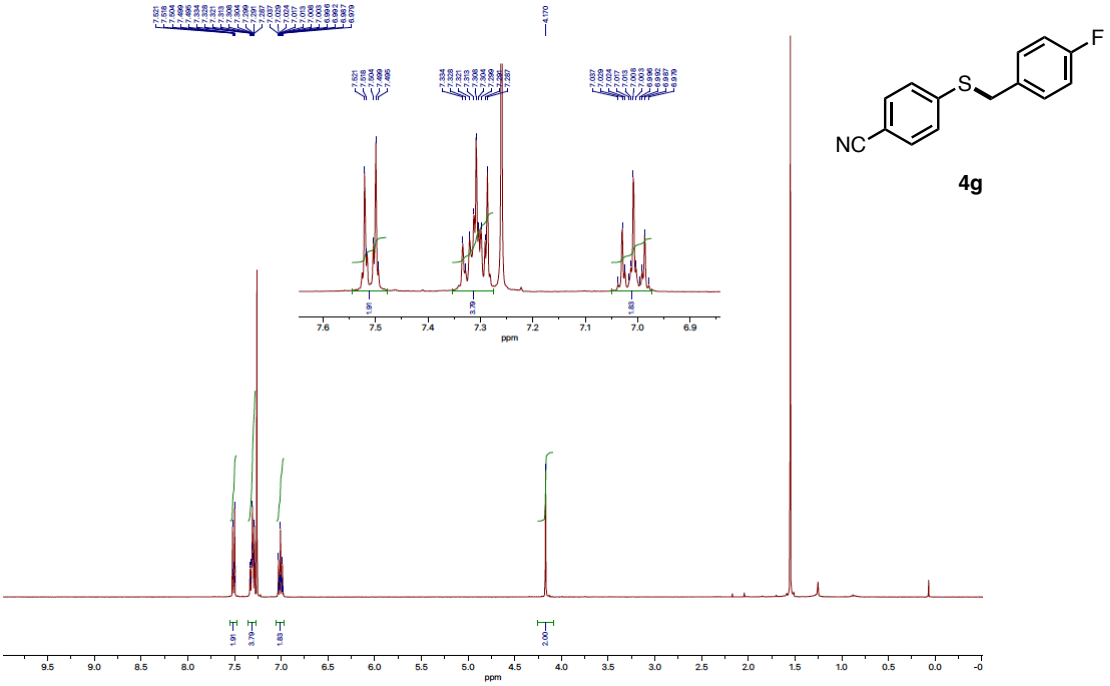

^{13}C{^{1}H} NMR (101 MHz, $CDCl_3$)

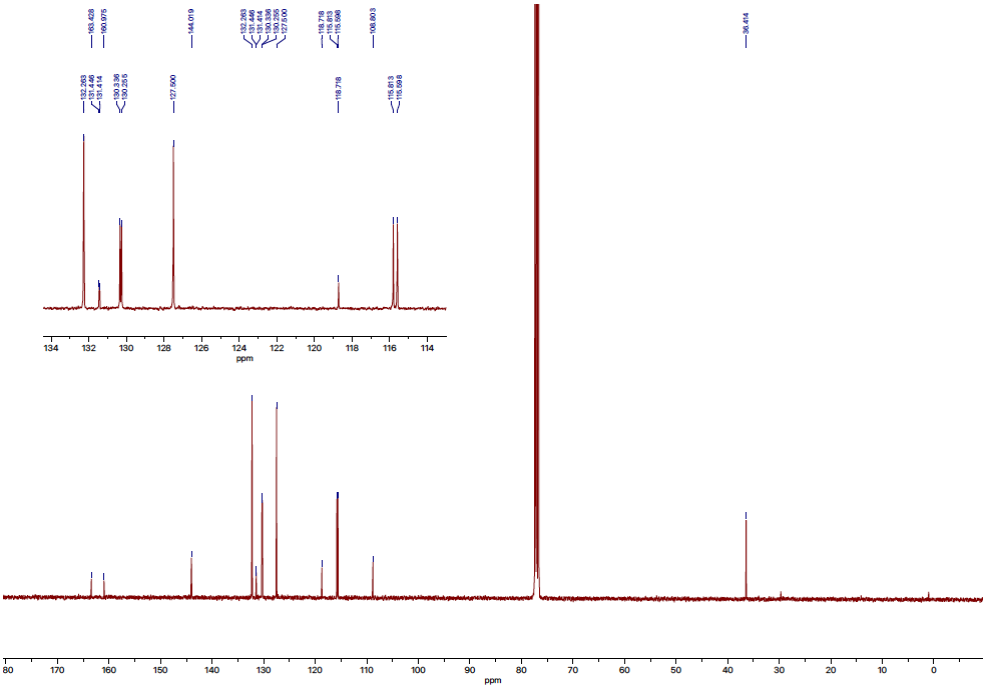

4h

^{1}H NMR (400 MHz, $CDCl_3$)

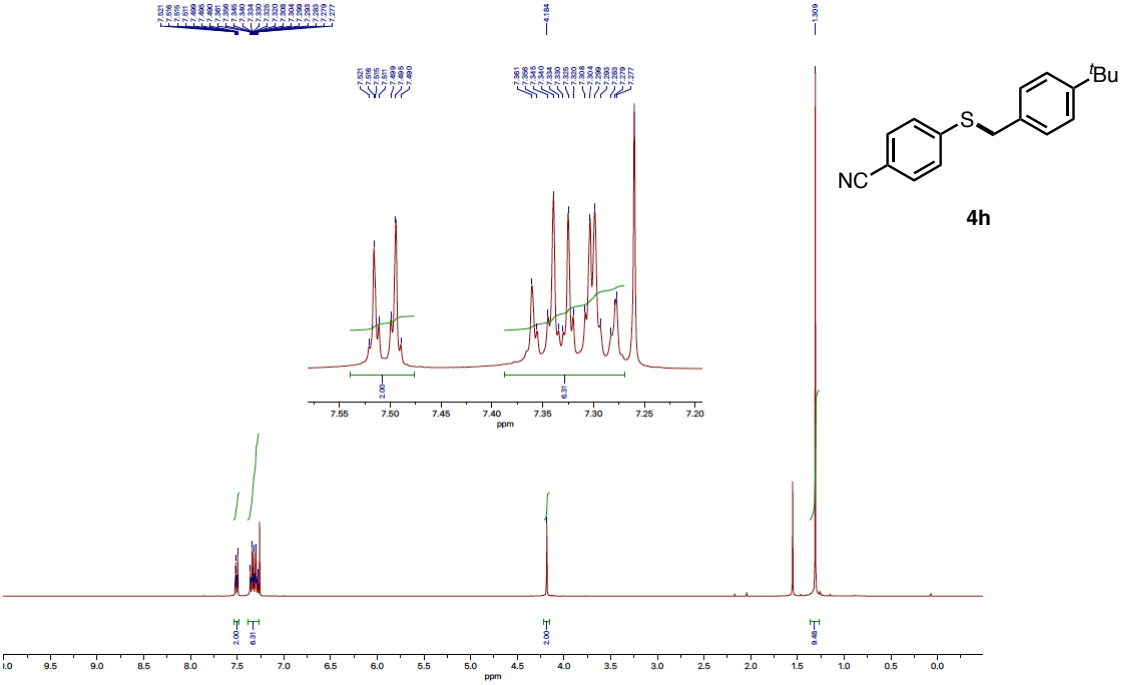

^{13}C{^{1}H} NMR (101 MHz, $CDCl_3$)

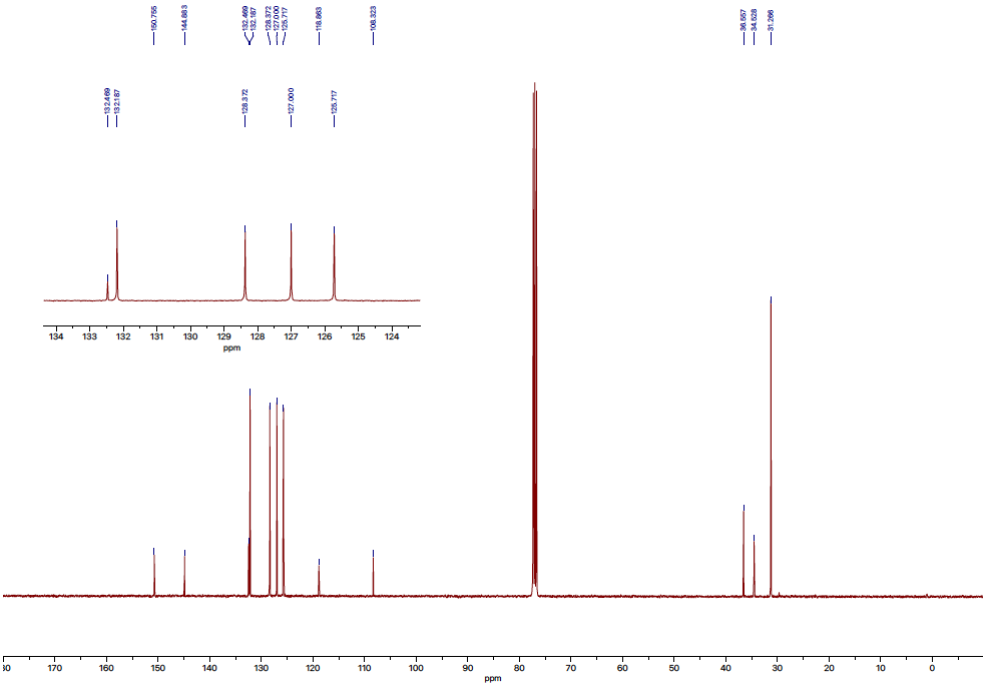

4i

^{1}H NMR (400 MHz, $CDCl_3$)

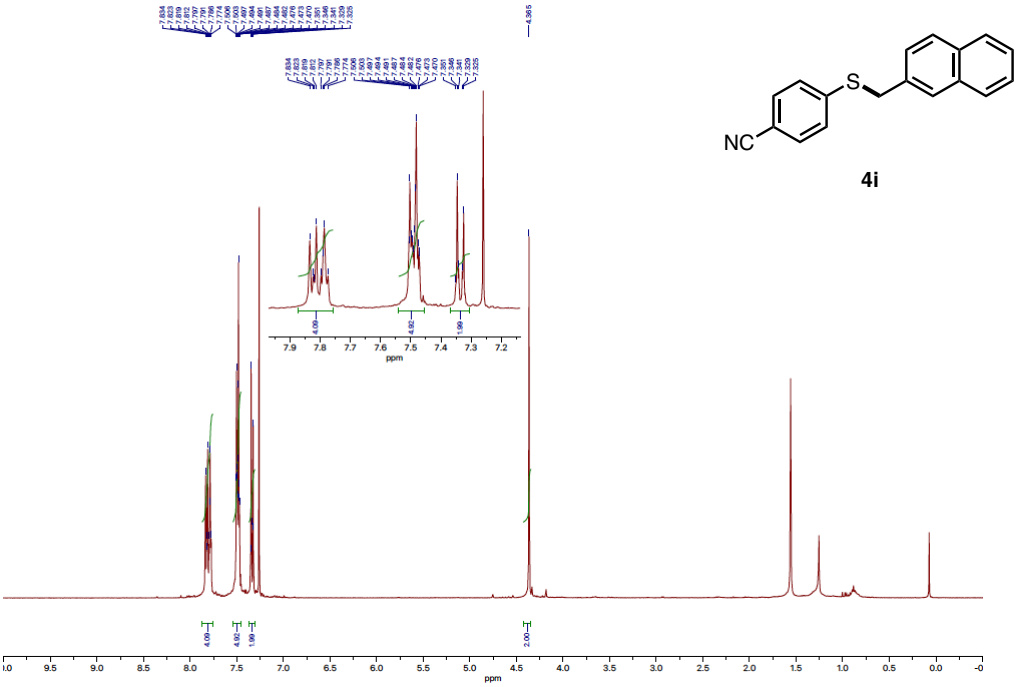

^{13}C{^{1}H} NMR (101 MHz, $CDCl_3$)

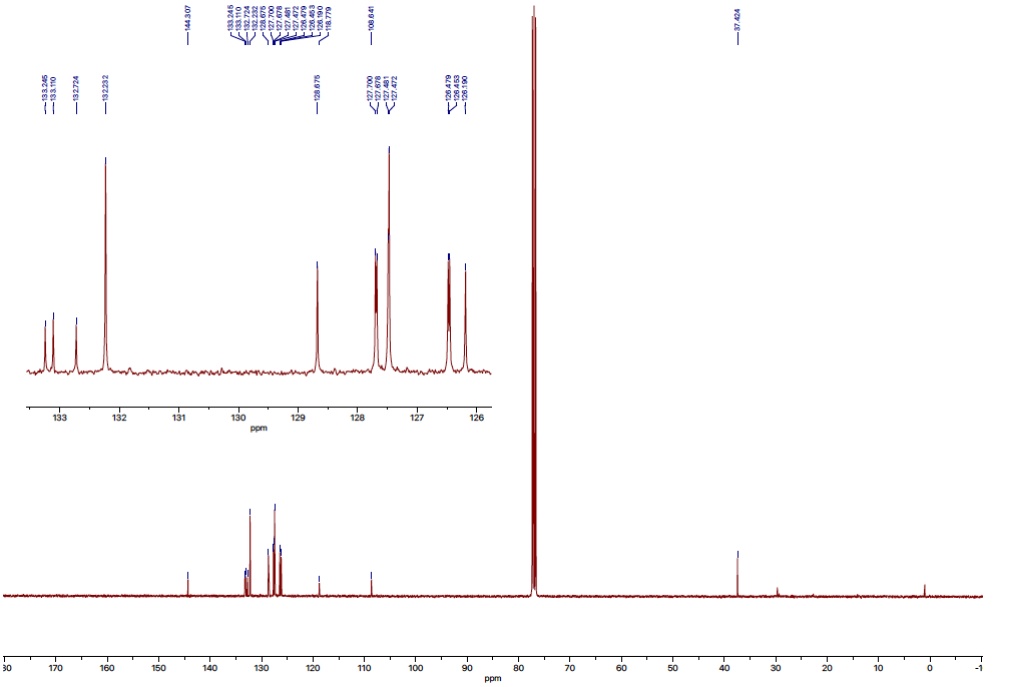

4j

^{1}H NMR (400 MHz, $CDCl_3$)

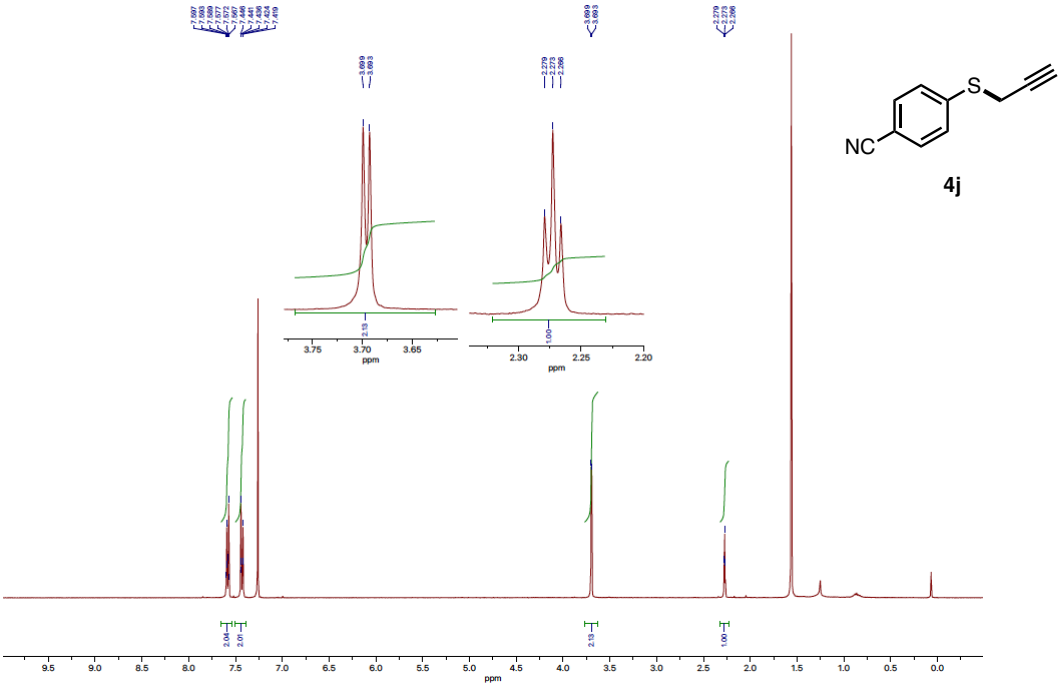

^{13}C{^{1}H} NMR (101 MHz, $CDCl_3$)